의학박사 학위논문

Study on the Mechanism of HBeAg Negative Chronic Infection and Liver Disease Progression via Type I Interferon Signaling in Patients with rt269I Polymorphisms on Polymerase Reverse Transcriptase of Hepatitis B Virus Genotype C

B 형 간염 바이러스 유전자형 C 의 역전사효소 내 rtL269I 변이주의 제 1 형 인터페론 신호전달을 통한 HBeAg 음성 감염 및 간질환 악화기전에 관한 연구

2020 년 2 월

서울대학교 대학원
의학과 미생물학전공

이 소 영

ABSTRACT

Background and Aims: Hepatitis B virus infection is a serious global health problem and causes life-threatening liver disease. In particular, genotype C shows high prevalence and sever liver disease compared with other genotypes. However, the underlying mechanisms regarding virological traits still remain unclear. This study investigated the clinical factors and capacity to modulate Type I interferon (IFN-I) between two HBV polymerase polymorphisms rt269L and rt269I in genotype C.

Methods: The clinical factors between rt269L and rt269I in 220 Korean chronic patients with genotype C2 infections were compared. The prevalence of preC mutations between rt269L and rt269I was compared using this cohort study and the GenBank database. For *in vitro* study, plasmid DNA encoding HBV genome were transiently transfected into hepatocytes, and HBV virions were infected using HepG2-hNTCP-C4 and HepaRG systems. In addition, hydrodynamic injection of HBV genome into mice tail were conducted for *in vivo* experiments.

Results: The clinical cohort study indicated that rt269I was related to HBV e antigen (HBeAg) negative serostatus, lower levels of HBV DNA and HBsAg, and disease progression compared to rt269L. Furthermore, the epidemiological study

showed that HBeAg negative infections of rt269I were attributed to a higher frequency of preC mutations at 1896 (G to A). *In vitro* and *in vivo* study also suggested that rt269I caused mitochondrial stress mediated STING dependent IFN-I production, resulting in decreasing HBV replication via the induction of heme-oxygenase-1. In addition, I also found that rt269I enhanced iNOS mediated NO production in an IFN-I dependent manner.

Conclusion: In this study, I found that there are two polymorphisms at polymerase RT region, rt269L and rt269I, in patients infected with genotype C, which is only found in genotype C. These data demonstrated that rt269I can contribute to HBeAg negative infections and liver disease progression in chronic patients with genotype C infections via mitochondrial stress mediated IFN-I production.

Keywords: hepatitis B virus; HBeAg negative infection; genotype C; mitochondrial stress; type I interferons

Student number: 2014-30594

CONTENTS

LIST OF TABLES

LIST OF FIGURES

LIST OF ABBREVIATIONS

HBV: Hepatitis B virus

S: Surface antigen

C: Core protein

Pol: Polymerase

X: X protein

RT: reverse transcriptase

cccDNA: covalently closed circular DNA

pgRNA: pre-genomic RNA

preC: pre-core

BCP: basal core promoter

CHB: chronic hepatitis B

CH: chronic hepatitis

LC: liver cirrhosis

HCC: hepatocellular carcinoma

IFN-I: type I interferon

HO-1: heme oxygenase

STING: Stimulator of interferon genes

IRSE: interferon stimulated response element

mtROS: mitochondrial ROS

NO: nitric oxide

iNOS: inducible nitric oxide synthase

8-OHdG: hydroxy-2′-deoxyguanosine

HDI: Hydrodynamin injection

INTRODUCTION

Viral hepatitis is a high-risk global health issue, leading to chronic infection that can cause fibrosis, liver cirrhosis (LC), hepatocellular carcinoma (HCC), and liver failure [1]. Compared to the life-threating infectious diseases, the number of deaths caused by viral hepatitis was comparable to deaths caused by tuberculosis, and higher than those caused by Human Immunodeficiency virus (HIV) and malaria. The number of deaths caused by HIV, tuberculosis, and malaria has declined, while the mortality caused by viral hepatitis has increased by 22% since 2000 [2]. Of the viral hepatitis, it was estimated that 350 million patients were chronically infected with hepatitis B virus (HBV) and 900,000 patients died [3], that accounted for 66% of the deaths caused by viral hepatitis. Furthermore, HBV infection is also a major public health problem in Korea. In 2015, it reported that liver cancer led the number of second-highest mortality among the entire cancer patients, and HBV infection accounted for 74% of the cause of liver cancer [4]. Although vaccines and therapeutic agents are currently available against HBV, the number of deaths caused by HBV has increased worldwide [5]. In these reasons, the alternative targets to HBV life cycle should be elucidated to effectively cure them.

HBV is an enveloped and partially double-stranded DNA virus, a species of genus *Orthohepadnavirus* and a member of the *Hepadnaviridae* family of viruses. The infectious virus particle, called Dane particle, is 42 nm in diameter. The HBV genome that is approximately 3.2 kb in length, and consists of four open reading frames (ORFs): surface antigens (S), core proteins (Cp), polymerase (Pol), and X proteins (X) [6]. Hepatitis B surface antigen (HBsAg) consists of small, medium and large protein, and Pol consists of

terminal protein (TP), spacer, reverse transcriptase (RT) and RNase H. HBV has tissue tropism to hepatocytes, and the viral life cycle starts when HBV attaches to cell surface receptor sodium taurocholate cotransporting polypeptide (NTCP) that is mostly found in the sinusoidal membrane of hepatocytes [7]. Following endocytosis, the viral memvrane fuses with the cell membrane, releasing the nucleocapsid containing the relaxed circular DNA (rcDNA) or double-stranded linear DNA (dsDNA) into cytoplasm and transferred to the nucleus [8]. After infecting the hepatocytes, the genomes from HBV are converted to covalently closed circular DNA (cccDNA) by host enzymes [9]. The cccDNA serves as a template to transcript sub-genomic RNA and pre-genomic RNA (pgRNA) that translate Cp and Pol. The synthesized Cp and Pol are encapsidated and are used to replicate more copies of genomes via reverse transcription activity of Pol. Surface and X proteins were translated from sub-genomic RNA and enveloped with nucleocapsid in Golgi-complex and finally released from the infected hepatocytes [9]. There are various therapeutic agents targeting in HBV life cycle and modulating virus-host interaction, such as nucleot(s)ide analogue agents and interferon-α [10]. HBV cccDNA is related to persistent infection cannot be completely eradicated by nucleot(s)ide analogue agents [11]. In these reasons, epigenetic regulation is necessary for the complete viral clearance from chronic hepatitis B (CHB) patients [12], that modulates innate immune response such as Type I IFN (IFN-I).

In pathogenesis, chronic HBV infection causes increased intracellular reactive oxygen species (ROS) and oxidative stress in host [13]. The increased levels of ROS induce a general inflammatory response that leads to a further increase in ROS and oxidative DNA damage, which cause progression of liver disease [14, 15]. In the responses

to ROS, heme-oxygenase-1 (HO-1) is strongly up-regulated and plays role in the cytoprotective enzyme via degradation of heme to generate carbon monoxide (CO), ferrous iron (Fe^{2+}), and biliverdin that is subsequently converted to bilirubin by biliverdin reductase [16]. Therefore, HO-1 interferes with chronic inflammation and enhances antiviral properties by its three active products [17]. In addition, HO-1 interacts with interferon regulatory factor-3 (IRF-3) to activate IFN-I response that is the first defense mechanism against viral infection [18].

IFN-I are large subgroup of interferon proteins and include IFN-α, -β, -ω, -κ, -τ, and -ζ, which bind to heterodimeric transmembrane receptor complex known as IFN-α receptors (IFNAR) that consist of IFNAR1 and IFNAR2 chains. IFN-I are produced by various cell types to elicit anti-viral responses [19] that are initiated after host recognition of viral pathogen-associated molecular patterns (PAMPs) through pattern recognition receptors (PRRs) [20] such as toll-like receptor (TLR), retinoic acid-inducible gene I (RIG-I)-like receptor, cytosolic DNA sensing receptor. They converge at the level of TBK1/IKKe that can phosphorylate transcription factors such as IRF3 and IRF7 to induce IFN-I [21]. In the second phase, the secreted IFN-I bind to IFNAR that triggers oligomerization and tyrosine phosphorylation of Janus kinase-1 (JAK-1) and tyrosine kinase-2 (TYK-2), which phosphorylate signal transducer and activator of transcription (STAT)-1 and -2 [22]. The activated STAT-1 and -2 heterodimerize with IRF-3 that translocate into the nucleus, where they bind to the interferon-stimulated response element (IRSE) and initiate transcription of ISGs [23]. In addition, IFN-I subsequently regulate other viral defense responses such as inducible nitric oxide synthase (iNOS) and APOBEC

enzymes [24, 25], which induce mutations such tryptophan codon (TGG) to a stop codon (TAG) on virus genome [26, 27] .

Cytosolic DNA is related to viral infection, invasion of intracellular bacteria, and damaged DNA as a cell intrinsic danger signal, which are mediated by cytosolic receptor cGAMP synthase (cGAS)-stimulator of interferon genes (STING) to induce IFN-I response [28]. Upon binding DNA, cGAS triggers reaction of GTP and ATP to form cyclic GMP-AMP (cGAMP) that binds to STING. STING phosphorylates IRF3 that can translocate into the nucleus to transcript ISGs [29]. This pathway plays a critical role in mediating immune defense against double-stranded DNA viruses. Hepatitis B virus DNA can be recognized by cGAS [30], and HBV pgRNA can be recognized by RIG-I, leading to induction of type I IFN [31]. However, HBV has developed various strategies to evade host IFN-I dependent innate immunity [32]. It has been reported that some HBV proteins such as HBsAg, HBV e antigen (HBeAg), and HBV virions can lead to inhibit TLR mediated IFN-I production [33]. In RNA sensing pathways, HBxAg and Pol can also negatively regulate RIG-I mediated antiviral responses [34, 35]. In addition, it has also been reported that HBV Pol can block IFN-I dependent antiviral pathways via the inhibition of STING dependent cytosolic DNA sensing pathways [36].

On the basis of an 8% divergence in HBV genome sequences, HBV has been characterized into 10 genotypes as A-J [37]. Various studies on HBV genotypes have reported that they have distinct pathogenic potential as well as distinct geographic and ethnic distributions [38], showing genotype A is predominant in sub-Saharan Africa, Northern Europe, and genotype D is common in Africa, Europe, Mediterranean countries. Among the 10 genotypes, genotypes B and C are widespread in Asia, being estimated more

than eighty-seven percent of patients. Although genotype B and C were showed in same high-endemic region by perinatal or vertical infection, two genotypes lead to distinctly different clinical outcomes [39]. Compared to genotype B, genotype C showed high HBV replication capacity, with high levels of HBV DNA in the serum [40, 41]. In addition, the tendency of chronicity was higher and more frequently developed into liver cirrhosis (LC) and hepatocellular carcinoma (HCC) in patients with genotype C than genotype B [42]. Furthermore, genotype C has low frequency of the well-known mutation, A1896 on pre-core region that stop translation of HBeAg, which can lead HBeAg positivity, and high frequency of basal core promoter T1762/A1764 that can cause severe disease progression and drug resistance [43]. These mutations can finally elicit strong resistance against nucleos(t)ide analogs and interferon therapy. However, the underlying mechanisms regarding distinct clinical and virological traits and distinct responses to IFN therapy between genotype C and genotype B remain unknown. Because genotype C has the great portion of chronic patients and worse disease progression, elucidation of their pathogenesis could lead to reduce various liver disease caused by HBV.

In previous studies, it has introduced that mutations on HBV genome can be highly associated with their pathogenesis of genotype C than other genotypes, such as P5H/L/T on C, W182* on S, and V5M and H94Y on X protein [44]. In addition, some mutations in the reverse transcriptase (RT) region of Pol related to HCC from genotype C infected patients [rtM80I, rtN139K/T/H and rtM204I/V] [45]. Although Pol is the protein that can not only regulate HBV genome replication but also overlapped with small surface antigen region, the mutation of them has not well studied. Furthermore, there are various anti-HBV drugs to block the Pol function, however, the effective drugs are still required.

Because Pol is essential for viral replication and effective target to develop anti-HBV drug, I tried to verify the correlation between mutations and disease progression in genotype C. In addition to HBV mutations, it has been reported that there are several genotype dependent polymorphisms in HBV RT regions, which are generally defined as having a frequency less than 10% versus wild type (**Table 1**). Of these, there are two polymorphisms at the Pol-269 site, rt269L (57.2%) and rt269I (42.8%), in patients with genotype C, in which two types are present with an almost similar ratio, but only rt269I is present as a major wild type in other genotypes.

In this study, I sought to investigate the clinical factors and capacity to modulate IFN-I between two HBV polymorphisms, rt269L and rt269I, in genotype C infected CHB patients. *In vivo* and *in vitro* study, I verified that rt269I infection causes mitochondrial stress that activates IFN-I signaling via cGAS-STING pathway. The activated IFN-I upregulate iNOS and APOBEC3G in the infected hepatocytes, suggesting higher frequency of G1896A mutation and HBeAg negative infection. These results suggested that the presence of two HBV Pol RT polymorphisms distinct only in HBV genotype C may play a very pivotal role in viral phenotypes, clinical outcomes, and worse responses to IFN therapy distinct in genotype C infections.

Table 1. Definition of HBV mutation and polymorphism at reverse transcriptase based on data

Pos (1-344)	Stanford HBV reverse transcriptase database								
	A (*n*=506)	**B (*n*=552)**	**C (*n*=734)**	**D (*n*=887)**	**E (*n*=311)**	**F (*n*=132)**	**G (*n*=22)**	**H (*n*=27)**	(
7	**D** A (17.8%) V (12.5%) T (10.6%)	**T** A (19.0%) S (1.4%)	**T** A (4.4%) I (0.8%)	**A** T (4.3%) V (2.2%) D (1.4%)	**T** S (0.7%)	**Y** H (18.7%) N (1.1%)	**T** D (5.6%)	**Y**	N
13	**H** Y (0.7%) N (0.2%)	**R** H (3.7%) L (2.2%)	**N** H (23.3%) S (3.6%)	**H** N (0.4%) Y (0.4%)	**H** Y (1.3%)	**H** Y (22.0%)	**H**	**H**	
55	**R** S (0.2%)	**R** H (0.3%)	**H** R (6.3%) Q (6.2%)	**R** K (0.1%)	**R**	**R** Q (0.8%)	**R**	**R**	
139	**Q** E (0.2%)	**N** H (1.8%) K (1.5%)	**H** K (1.4%) T (0.7%)	**N** S (0.8%) T (0.5%)	**N** D (1.3%)	**N** H (0.8%)	**Q**	**N**	
269	**I** L (2.5%)	**I** L (2.0%)	**I** L (43.0%)	**I** L (2.6%)	**I**	**I** L (5.7%)	**I**	**I**	
337	**N** D (2.1%) H (0.5%)	**N** T (9.2%) H (2.5%)	**N** H (19.5%) T (0.9%)	**N** T (3.5%) H (1.3%)	**N** T (2.7%) D (2.3%)	**N** H (8.0%)	**N**	**N** T (3.7%)	

MATERIALS AND METHODS

1. Patients

For this study, serum samples were collected from 410 patients chronically infected with HBV and the amino acid at 269th on RT region was identified by direct sequencing method. In 190 patients of these, their polymorphisms could not be identified by sequencing analysis due to lack of sensitivity. However, 220 patients could be identified into their polymorphism, rt269L or rt269I types and selected for this study. To elucidate the correlation between the polymorphism of 269th amino acid and the characteristics of disease, their clinical factors and polymerase RT regions were assessed. This report was approved by the Institutional Review Board of Konkuk University Hospital (KUH-1010544) and Seoul National University Hospital (IRB-1808-067-965).

2. HBV DNA extraction and PCR amplification for polymerase RT region

For this cohort study, HBV DNA was extracted from the serum of patients using a QIAamp DNA Blood Mini kit (QIAGEN, Hilden, Germany) and dissolved in Tris-EDTA buffer (10 mM Tris-HCl, 1 mM ethylenediaminetetraacetic acid, pH 8.0). First-round PCR was performed using primers POL-RT1 and the amplicon was used as templates for second-round PCR using primers. The PCR products were subject to direct sequencing analysis.

3. HBV genotyping

The 1,032-bp polymerase RT sequences were examined by direct sequencing and were compared to the sequences of the reference strains representing each of the genotypes (A-H including the C strains) obtained from GenBank. The sequences of the RT region were compared via phylogenetic/molecular evolutionary analysis using MEGA version 7.0 and MrBayes version 3.2.7. Phylogenetic trees were obtained using the Maximum-likelihood method (1,000 bootstrap replicates) and Bayesian method, and the mean genetic distances were estimated using Kimura two-parameter model.

4. Plasmid and site-directed mutagenesis

The pHBV-1.2x (GenBank accession No. AY641558) containing genotype C HBV full-length genome was used for site-directed mutagenesis to generate polymerase RT mutant DNA constructs using an *i*-pfu kit (iNtRON, Seongnam, Korea). Mutagenesis was performed using the primers rt269I based on rt269L construct. To exclude CMV promoter, HBV full genome constructs were cut by restriction enzymes and prepared for linear formed genome.

5. Cell culture and transfection

Human hepatocellular carcinoma HepG2 cells and mouse hepatoma Hepa-1c1c7 purchased from the Korean Cell Line Bank (KCLB, Seoul, South Korea) were grown in minimum essential medium (MEM) supplemented with 10% fetal bovine serum (FBS), 100 μg/ml of penicillin-streptomycin, and 25 mM HEPES at 37℃ in a humidified environment containing 5% CO_2. pHBV-1.2x containing genotype C HBV full-length

genome (2.5 μg) was transiently transfected using Lipofectamine 3000 (Invitrogen, Carlsbad, CA, USA). To normalize the transfection efficacy, pSV-β-Galactosidase (0.25 μg) was co-transfected, and the enzyme assay was accompanied using β-Galactosidase Enzyme Assay System with Reporter Lysis buffer (Promega, Madison, WI, USA), following the manufacturers' protocol.

6. *In vivo* assay and hydrodynamic injection

Female C57BL/6 mice (7 weeks old) were hydrodynamically tail-vein injected with HBV DNA (10 μg) per 8% of mouse body weight within 30 seconds. All of the animal experiments were approved by the Institutional Animal Care and Use Committee (IACUC) of Seoul National University College of Medicine (SNU-170308). Mice were sacrificed on 4, 7, and 16 days after HBV-encoding DNA injection, and liver and serum were used to analyze gene expression of ISGs and HBV viral factor, respectively.

7. Enzyme-linked immunosorbent

To measure the HBV antigens in the blood serum or culture supernatant, ELISA was performed for HBsAg (Biokit, Barcelona, Spain) and HBeAg (AccuDiag, Oceanside, CA, USA) according to the manufacturers' instructions. The concentration of mouse and human IFN-β was measured with ELISA kit purchased from Biolegend (San Diego, CA, USA) and PBL assay Science (Piscataway, NJ, USA), respectively. According to the manufacturer's procedure.

8. Covalently closed circular DNA extraction and real-time polymerase chain reaction

The pHBV-1.2x with rt269L or rt269I were digested with restriction enzyme SmaI to remove CMV promoter, and the linear DNA (2.5 μg) were transfected using lipofectamine 3000 following manufacture's instruction. The transfected cells were lysed with lysis buffer (50 mM Tris-HCl, pH7.4, l mM EDTA, and 1% NP-40), and the nuclei were collected via centrifugation and incubated with nucleus lysis buffer (10 mM Tris-10 mM Tris-HCl, 10 mM EDTA, 150 mM NaCl, 0.5% SDS, and 0.5 mg/ml protein K). The nucleic acids were purified via ethanol precipitation and treated with 10 U Plasmid-Safe ATD dependent DNase I (PSAD, Epicentre, Madison, WI, USA). The cccDNA was purified by PCI and ethanol precipitation and quantified via real-time PCR using SYBR and primers cccDNA-F and cccDNA-R (**Table 2**).

Table 2. PCR primers used for this study.

Primers	Forward	Reverse
POL-RT1	CAG CCT ACT CCC ATC TCT CCA CCT CTA AG	GCT CCA GAC CGG CTG CGA
POL-RT2	CCT CAG GCC ATG CAG TGG AA	GTA TGG ATC GGC AGA GGA
rt269I-C	GAA CAT ATT GTA CAA AAA ATC AAG CAA TGT TTT CGG AAA	TTT CCG AAA ACA TTG CTT C
pgRNA	GGT CCC CTA GAA GAA GAA CTC CCT	CAT TGA GAT TCC CGA GAT
cccDNA	CCG TCT GTG CCT TCT CAT	CAC AGC TTG GAG GCT TGA
mouse APOBEC3G	CCC CTG TTT CGA ATG TGC A	TGG TGT GTA GCC AGG AAC C
mouse IFN-α	TCT GAT GCA GCA GGT GGG	AGG GCT CTC CAG ACT TCT C
mouse IFN-β	GCA CTG GGT GGA ATG AGA CT	AGT GGA GAG CAG TTG AGG
mouse iNOS	GGC AGC CTG TGA GAC CTT TG	GCA TTG GAA GTG AAG CGT
human APOBEC3G	ACA ACA GGT AGT AGG CGA CA	CCA ACA GTG CTG AAA TTC C
human IFN-β	AGC AAG TTG TAG CTC ATG GAA	ACA ACA GGT AGT AGG CGA C
human RIG-I	GGA CGT GGC AAA ACA AAT CAG	GCA ATG TCA ATG CCT TCA TC
human ISG-15	AGC TCC ATG TCG GTG TCA G	GAA GGT CAG CCA GAA CAG
human HO-1	ACA TCT ATG TGG CCC TGG AG	TGT TGG GGA AGG TGA AGA
human iNOS	GTT CTC AAG GCA CAG GTC TC	GCA GGT CAC TTA TGT CAC T
mouse/human 18S rRNA	AGT CCC TGC CCT TTG TAC ACA	CGA TCC GAG GGC CTC ACT A

9. Total RNA extraction and real-time polymerase chain reaction (qRT-PCR)

Total RNA was extracted from the transfected cells or mouse liver tissue using TRIzol and the target genes were amplified using SensiFAST SYBR Lo-ROX One-Step kits (BioLine, London, UK). The transcription level was analyzed using qRT-PCR with sets of primers (**Table 2**) and housekeeping gene 18S ribosomal RNA was used as an internal control.

10. IFN-I luciferase reporter assay

Cell culture supernatants from transfected cells were overlaid on top of HEK293 IFN reporter cells containing ISRE-luciferase construct [46] and incubated for 4 hours. The reporter cells were lysed in passive lysis buffer (Promega, Madison, WI, USA) for 30 minutes at room temperature, mixed with firefly luciferin substrate (Promega, Madison, WI, USA), and measured using an illuminometer (Beckman Coulter Inc., Fullerton, CA, USA).

11. IFN-I signal block assay

HepG2 cells were pre-treated with 10 μg of anti-IFNAR2 antibody (PBL assay Science, Piscataway, NJ, USA) and AZD1480 (Sigma, St. Louis, MO, USA) in MEM supplemented with 2% of FBS and transfected with pHBV-1.2x DNA constructs. STING-siRNA were co-transfected with pHBV-1.2x DNA constructs, following the manufacturers' procedures (Santa Cruz Biotechnology, Dallas, TX, USA, and Thermo-Fisher Scientific, Waltham, MA, USA).

12. Preparation of HBV from transiently transfected cells and Infection assay

For an infection study, culture supernatant of HepG2 cells, transiently transfected with 1.2x-rt269L or rt269I type of HBV plasmid, was collected. The supernatant was cleared through a sterile 0.45-μm pore size filter and precipitated with 6% polyethylene glycol (PEG) 8000 overnight. The media were ultracentrifuged and the collected pallet was resuspended in PBS containing 15-25% FCS. After quantification by qPCR, 3 X 10^9 HBV genome equivalent per milliliter was aliquoted and stored at -80 ℃. HepaRG and HepG2-hNTCP-C4 cells were seeded in 12-well plates. Infection assay was performed with the concentrated virus in the presence of 4% PEG8000 at 37 ℃ for 20h. HepaRG was purchased from BIOPREDIC International (HPR116) and HepG2-hNTCP-C4 was kindly provided by Dr. Koichi Watashi (National Institute of Infectious Disease, Tokyo, Japan).

13. Flow cytometry and Confocal analysis

The mtROS were stained with MitoSox (5 μM), and analyzed by flow cytometry (LSRII, Becton Dickinson) and confocal microscope (Confocal-A1, Nikon). DAPI was used to stain nuclei and the cells were mounted in mounting medium (VECTASHIELD Antifade Mounting Medium, H-1000). The images were captured using a 100x oil immersion objective lens.

14. 8-OHdG ELISA assay

Genomic DNA was extracted from the transfected cells using QIAamp Blood DNA extraction kit (QIAGEN, Hilden, Germany). For the detection of 8-hydroxy-2′-deoxyguanosine (8-OHdG) activity, a competitive ELISA for 8-OHdG analysis kit

(OxiSelect Oxidative DNA Damage ELISA kit, Cell Biolabs, San Diego, CA, USA) was used according to the manufacture's protocol.

15. Measurement of NO_2^- and NO_3^- levels

The produced NO was measured using culture supernatants from the transfected cells using a colorimetric Nitrite/Nitrate Assay Kit (Sigma, St. Louis, MO, USA) according to the manufacturer's instructions, and measured the absorbance at 540 nm in microplate reader (TECAN).

16. Statistical Analyses

For the cohort study, statistical analysis was performed using SPSS Software (IBM SPSS version 23.0.0.0 Inc., Chicago, USA). Categorical variables were analyzed using Multivariate Analysis of Variance (MANOVA). Independent *t*-test was used to compare continuous variables. Tests were two-sided.

Experimental data were analyzed using Graphpad Prims 5 (GraphPad Software, La Jolla, CA, USA). All experiments were independently repeated three times and the statistical analyses were indicated in the figure legends. The p value of statistical significance was set at either; $^{*}p < 0.05$; $^{**}p < 0.01$; $^{***}p < 0.001$.

RESULTS

1. rt269I was related to enhanced disease progression in a Korean cohort with genotype C infections.

In the web page "HBV RT: Mutation prevalence according to genotype and treatment" (https://hivdb.stanford.edu/HBV/DB/cgi-bin/MutPrevByGenotypeRxHBV.cgi.), the mutation prevalence or polymorphisms of the entire HBV RT region were analyzed according to the genotypes and antiviral drug treatments (**Table 1**). A comparison of all of the 344 codons of RT found one unique genotype C site at the 269th codon of RT, in which both types, one for rt269L encoding leucine and the other for rt269I encoding isoleucine, were present in patients infected with genotype C at frequencies of 57.2% and 42.8%, respectively. Although rt269 codon is located at the outer region of overlapped HBsAg, polymorphism of rt269 cannot lead to HBsAg amino acid change, not affecting the performance of the HBsAg kit or immunoblotting data. There were no other polymorphisms in patients infected with genotype C exceeding 10% of the total frequency. Therefore, I postulated that the polymorphism at the 269th codon of RT may play an important role in the clinical outcomes and pathogenesis of genotype C infections. To address this issue, I analyzed the 269th codon polymorphisms of 220 patients in the Korean cohort with genotype C via direct sequencing of the RT region (**Figure 1)** and compared their clinical factors between rt269L and rt269I.

Overall, 138 patients (62.7%) and 82 patients (37.3%) were infected with rt269L and rt269I, respectively (**Table 3**). Interestingly, I found there were several patients mixed with

both rt269L and rt269I in sequencing data, maybe due to quasi species generation. In these cases, I determined their polymorphisms types into one reflecting dominance in sequencing data.

Interestingly, there were distinct disparities in some clinical factors between the patients with rt269L and rt269I (**Table 3**). The patients with rt269I had significantly lower levels of HBV DNA and HBsAg, HBeAg negative infection, and liver disease progression based on immune response against HBV [47]. These data suggested that both rt269L and rt269I on the RT region may be key factors determining clinical outcomes regarding disease progression and HBeAg negative infection in genotype C infected patients.

A

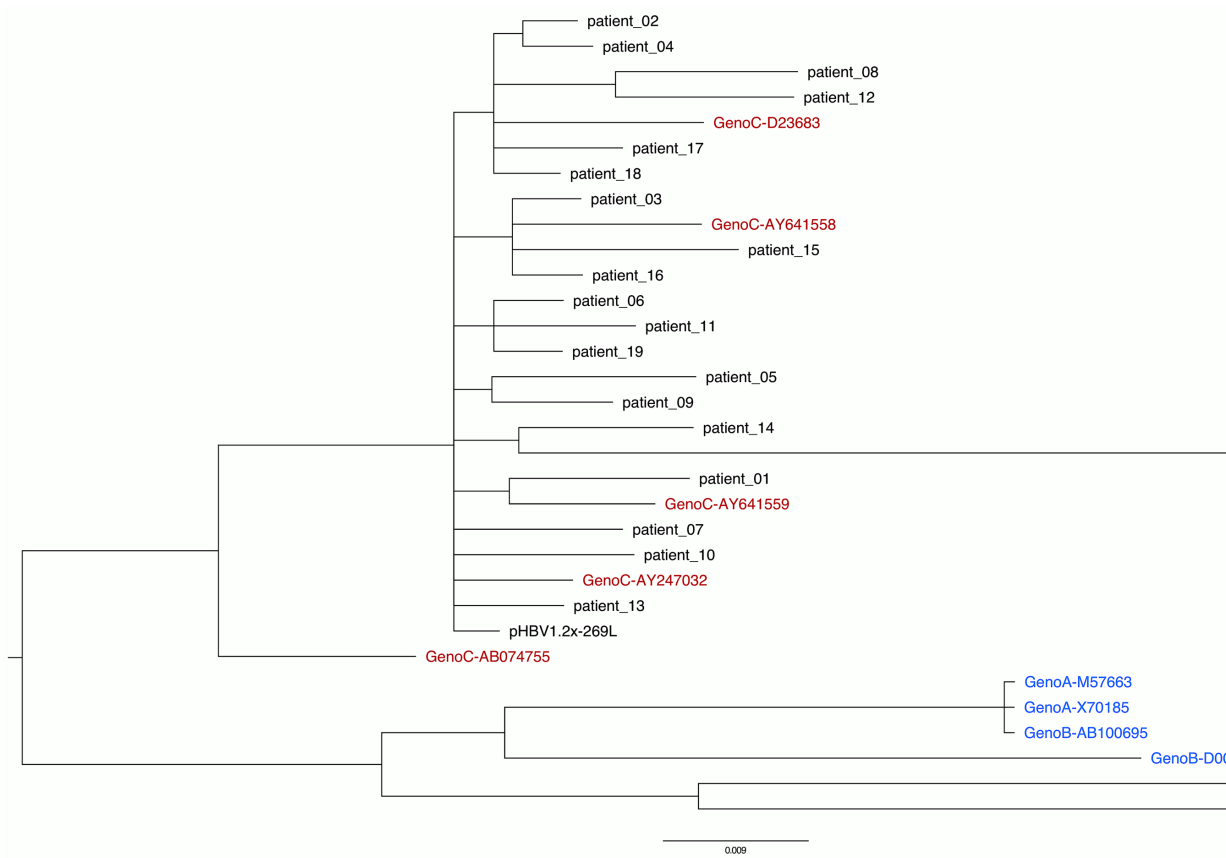
patient_02
patient_04
patient_08
patient_12
GenoC-D23683
patient_17
patient_18
patient_03
GenoC-AY641558
patient_15
patient_16
patient_06
patient_11
patient_19
patient_05
patient_09
patient_14
patient_01
GenoC-AY641559
patient_07
patient_10
GenoC-AY247032
patient_13
pHBV1.2x-269L
GenoC-AB074755
GenoA-M57663
GenoA-X70185
GenoB-AB100695
GenoB-D0
0.009

B

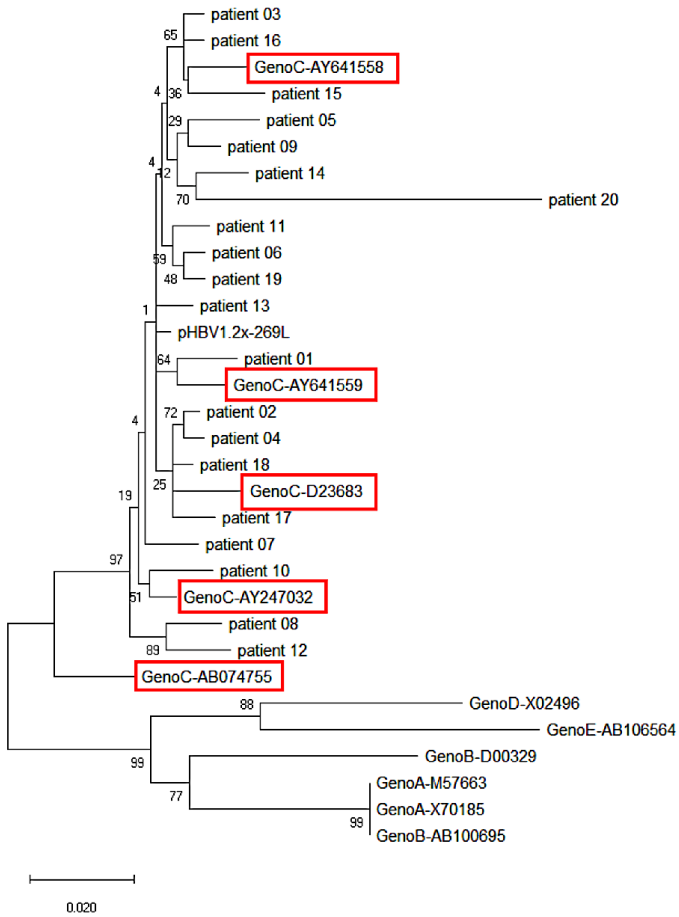

Figure 1. Phylogenetic analyses of 1,032-bp polymerase RT sequences showed that the representative 20 patients used in cohort study belonged to genotype C. The RT sequences were aligned using MEGA7 and the phylogenetic trees were constructed using Bayesian (**A**) and Maximum likelihood (**B**) method. The bootstrap values were calculated from 1,000 replications, and burn in was set at 25% of samples. The bars indicate numbers of substitutions per nucleotide position.

Table 3. Comparison of the clinical features between patients infected with the two types of genotype C, rt269L and rt269I.

Clinical factors	**rt269L (*n*=138)**	**rt269I (*n*=82)**	***p*-value**
CH:HCC	92:46	46:36	ns
Sex, men	63.04%	64.63%	ns
HBeAg negative	28.99%	52.44%	**
AST/ALT	1.16±0.78	1.42±1.43	ns
HBV-DNA (log10 copies/ml)	6.47±1.71	5.75±1.62	**
HBsAg (log10 IU/ml)	3.74±0.61	3.41±0.71	***
Age (years)	42.04±12.45	45.89±12.61	*
Bilirubin (mg/dL)	0.99±0.91	1.37±.1.71	*
Albumin (g/dL)	4.01±0.58	3.95±0.63	ns
Prothrombin time (INR)	1.11±0.18	1.14±0.18	ns
Platelet (10^9/L)	169.93±63.74	168.43±81.93	ns
Fibrosis-4 score	4.05±7.96	4.45±5.42	ns
Disease phase †			
1	18.12%	6.10%	
2	52.90%	41.46%	**
3	24.64%	43.90%	
4	4.35%	8.54%	

CH, chronic hepatitis; HCC, hepatocellular carcinoma; AST, aspartate aminotransferase; ALT, alanine transaminase.

†1. Immune-tolerant. 2. Immune-clearance. 3. HBeAg negative CHB. 4. Inactive carrier.

Continuous variables were tested using the chi-squared test and categorical variables were analyzed using Student's *t*-test. ns, non-significant; $^{*}p<0.05$; $^{**}p<0.01$; $^{***}p<0.001$

2. The higher frequency of preC mutation (G1896A) in patients with rt269I infections was responsible for the higher frequency of HBeAg negative infections.

Of the various HBV mutations, G1896A mutations on the pre-core region (preC mutation) and A1762T/G1764A double mutations on the basal core promoter (BCP) lead to HBeAg negative infection that are significantly related to liver disease progression [48]. To verify whether these mutations are associated with distinct clinical factors of genotype C infections between rt269L and rt269I, their mutation rates were compared not only to chronic infectious patients in the cohort study, but also to the reference strains in GenBank (**Table 4**). In double mutations in BCP, only the G1764A mutation, but not the A1762T, was significantly prevalent in patients with rt269I and in GenBank. In addition, the rate of G1986A preC mutation was significant higher in patients with rt269I (49.61%) than those with rt269L (28.83%, $p<0.01$). These results suggested that the high frequency of G1986A preC mutation is responsible for HBeAg negative infections in patients with genotype C rt269I infections.

Table 4. The frequencies of BCP and preC mutations between rt269L and rt269I in a Korean cohort and

Mutation		Nucleotide	Clinical isolates			Ref
			rt269L (*n*=115)	rt269I (*n*=69)	*p*-value	rt269L (*n*=111)
BCP mutation	A1762T	A	47 (40.87%)	23 (33.33%)	ns	31 (27.93%)
		T	68 (59.13%)	46 (66.67%)		80 (72.07%)
	G1764A	G	44 (38.26%)	16 (23.19%)	*	29 (26.13%)
		A	71 (61.73%)	53 (76.81%)		82 (73.87%)
preC mutation	G1896A	G	83 (72.17%)	33 (47.83%)	***	79 (71.17%)
		A	32 (27.83%)	36 (52.17%)		32 (28.83%)

BCP, basal core promoter; preC, pre-core

Continuous variables were tested using the chi-squared test. ns, non-significant; $^{*}p<0.05$; $^{**}p<0.01$; $^{***}p<0.001$

3. rt269I led to lower levels of HBV replication *in vitro* and *in vivo* experiments.

The clinical and epidemiologic data suggested there may be differences in the HBV replication capacity between rt269I and rt269L infections. To verify this hypothesis, I performed *in vivo* and *in vitro* study with genotype C HBV full genome constructs with leucine or isoleucine at the 269th amino acid on the RT region. HBV replications between rt269I and rt269L infections were analyzed via *in vivo* and *in vitro* studies. The secreted HBsAg and HBV DNA was greatly increased in the serum from the mice infected with rt269L. However, rt269I showed relatively lower HBV replication levels (**Figure 2A and B**). As shown in the *in vivo* study, the secreted HBsAg and HBeAg levels also decreased in HepG2 cells transfected with rt269I (**Figure 3A** and **B**). These replicative capacities were also examined in HepG2 cells via transient transfection of the linearized HBV DNA constructs (**Figure 3C** and **D**), in which CMV promoter was deleted [49]. Intracellular intermediates of HBV amplification were also examined by Southern blotting, which indicated that double-stranded (DS) and single-stranded (SS) DNA were significantly reduced in rt269I at 48 hours post-transfection. (**Figure 4A**). In addition, the HBV capsid form that is an intermediate of HBV amplification was significantly reduced in rt269I at 24 hours after transfection (**Figure 4B**). Similarly, rt269I also showed decreased pgRNA levels and cccDNA levels (**Figure 4C** and **D**). Together, I found that rt269I reduces HBsAg, HBeAg, capsid form, cccDNA, and pgRNA that is observed in HBV life cycle, compared to rt269L.

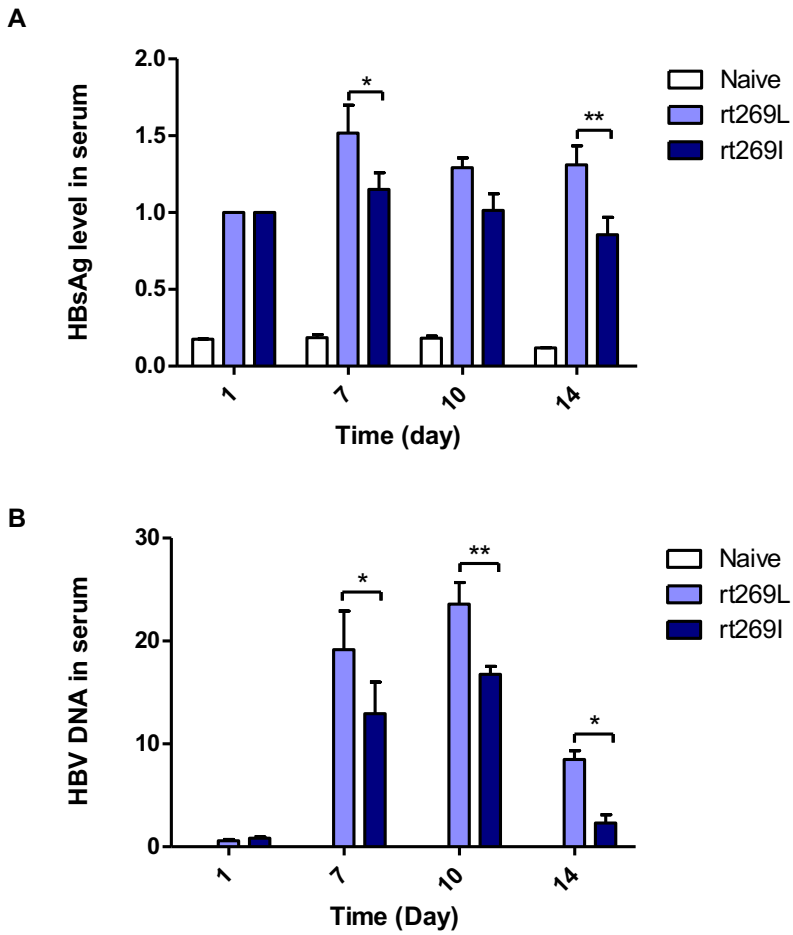

Figure 2. The viral replication of rt269I was restricted *in vivo* infection model. Both HBV-encoding DNA (10 μg) and pSV-β-Galactosidase (1 μg) was injected by hydrodynamic tail vein injection into C57BL/6 mice (n=5). **(A)** The secreted HBsAg in serum was measured by ELISA. **(B)** HBV DNA in serum were determined by qPCR and normalized with *β-Galactosidase*. Two-way ANOVA were used. $^{*}p<0.05$, $^{**}p<0.01$, $^{***}p<0.001$.

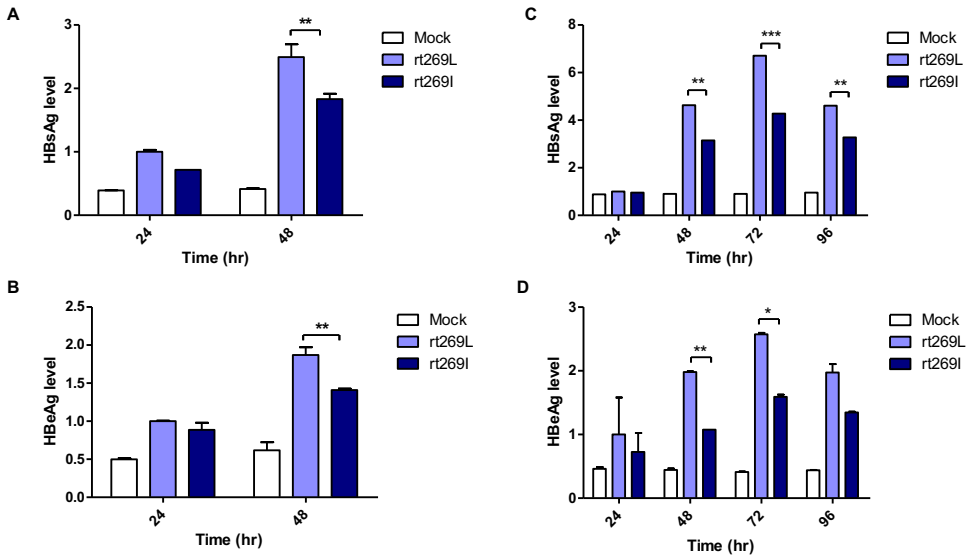

Figure 3. rt269I reduced viral replication *in vitro* analyses. (A and B) pHBV-1.2x-rt269L and -rt269I were co-transfected with pSV-β-Galactosidase into HepG2 cells and the replicative capacities were analyzed. The level of secreted HBsAg **(A)** and HBeAg **(B)** were detected using ELISA. **(C and D)** The plasmid DNA were restricted by *SmaI* digestion to remove CMV promoter. The linearized DNA was transiently transfected to HepG2 cells and the levels of secreted HBsAg **(C)** and HBeAg **(D)** were analyzed using ELISA. Data were normalized by β-Galactosidase assay, and represent mean±S.D. Two-way ANOVA were used. $^{*}p<0.05$, $^{**}p<0.01$, $^{***}p<0.001$.

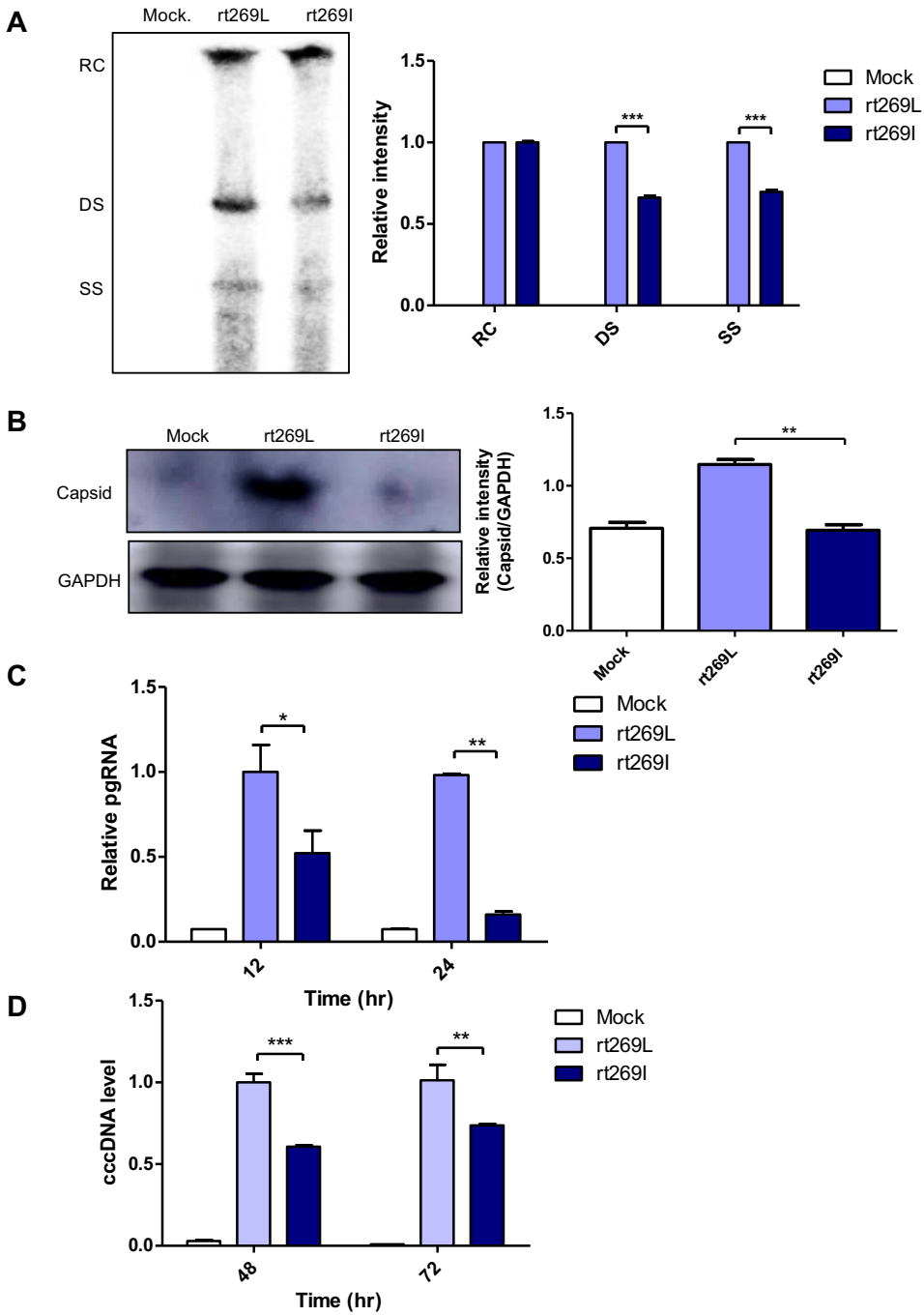
A
Mock.
rt269L
rt269I
RC
DS
SS
Relative intensity
1.5
1.0
0.5
0.0
***
***
RC
DS
SS
Mock
rt269L
rt269I
B
Mock
rt269L
rt269I
Capsid
GAPDH
Relative intensity (Capsid/GAPDH)
1.5
1.0
0.5
0.0
**
Mock
rt269L
rt269I
C
Relative pgRNA
1.5
1.0
0.5
0.0
*
**
12
24
Time (hr)
Mock
rt269L
rt269I
D
cccDNA level
1.5
1.0
0.5
0.0
***
**
48
72
Time (hr)
Mock
rt269L
rt269I

Figure 4. The viral replication of rt269I was reduced *in vitro* transient transfection system. pHBV-1.2x-rt269L and -rt269I were co-transfected with pSV-β-Galactosidase into HepG2 cells and the replicative capacities were analyzed. **(A)** HBV DNA was compared via Southern blotting at 48 hours post-transfection. **(B)** Western blot analyses of intracellular capsid forms were performed by using anti-HBcAg antibody on naïve gel at 24 hours after transfection. **(C)** The translation mediates pgRNAs were detected by qRT-PCR. **(D)** The linearized DNA was transiently transfected into HepG2 cells. The intermediates of transcripts cccDNA were determined using qPCR. Data were normalized to β-Galactosidase enzyme assay. Data represent mean±S.D. One- and two-way ANOVA were used. $^{*}p<0.05$, $^{**}p<0.01$, $^{***}p<0.001$.

4. Hepatocytes activated IFN-I signaling against rt269I infection.

Since IFN-I medicate antiviral effects by up-regulating APOBEC3G that hypermutate the HBV genome, I postulated that rt269I can enhance IFN-I mediated APOBEC3G signaling in infected hepatocytes and finally led to the higher frequency of G to A mutations on preC and BCP in patients with rt269I. To address this issue, I compared the gene expression of two representative IFN-I genes, INF-α and INF-β, and interferon stimulated genes, ISG-15, RIG-I, and APOBEC3G that are induced by an IFN-I signal [50]. The mRNA levels of APOBEC3G, ISG-15, RIG-I, IFN-α, and IFN-β were significantly enhanced in the mice infected with rt269I on 4 days post-infection (**Figure 5**). In the same manner as shown in *in vivo* assays, the transcription levels of APOBEC3G and IFN-I-related genes, such as ISG-15, RIG-I, IFN-α, and IFN-β, were also induced in HepG2 cells transfected with rt269I at 12 hours after transfection (**Figure 6**). To evaluate the upstream genes of the IFN-I signaling pathway, the activation or expression of STAT-1, IRF-3 and the STING genes [51, 52] were analyzed using Western blotting at 48 hours post-transfection (**Figure 7A**). rt269I activated STAT-1, IRF-3 and up-regulated STING in protein level. The secreted IFN-β was also assessed by ELISA and treating culture supernatant from the transfected cell onto HEK293 with luciferase construct under an interferon stimulated response element (ISRE) promoter [46]. As the results of activated IFN-I signal, the secreted IFN-I was significantly induced in cells transfected with rt269I at 24 hours post-transfection (**Figure 7B** and **C**). These results were consequently shown in the Huh-7 and Huh-7.5 cells defective in RIG-I

signaling at 24 hours after transfection (**Figure 8A** and **B**). It suggests that the enhancing effect of IFN-I found in rt269I may be due to pathways other than the RIG-I dependent pathway. Interestingly, rt269I enhanced IFN-I, even compared to genotype A wild type with the isoleucine at the 269th amino acid of RT at 24 hours after transfection (**Figure 8C**), suggesting that the trait capable of IFN-I induction as found in rt269I may be specific to genotype C. In addition, the HBV encoding DNA was also transfected into mouse hepatoma cell Hepa1c1c-7 and IFN-β was measured assessed by ELISA (**Figure 8D)**. Consistent with human hepatocellular cells, mouse hepatocytes transfected with rt269I produced enhanced IFN-β production, compared to rt269L. Together, the data indicated that rt269I enhances IFN-I production in hepatocytes.

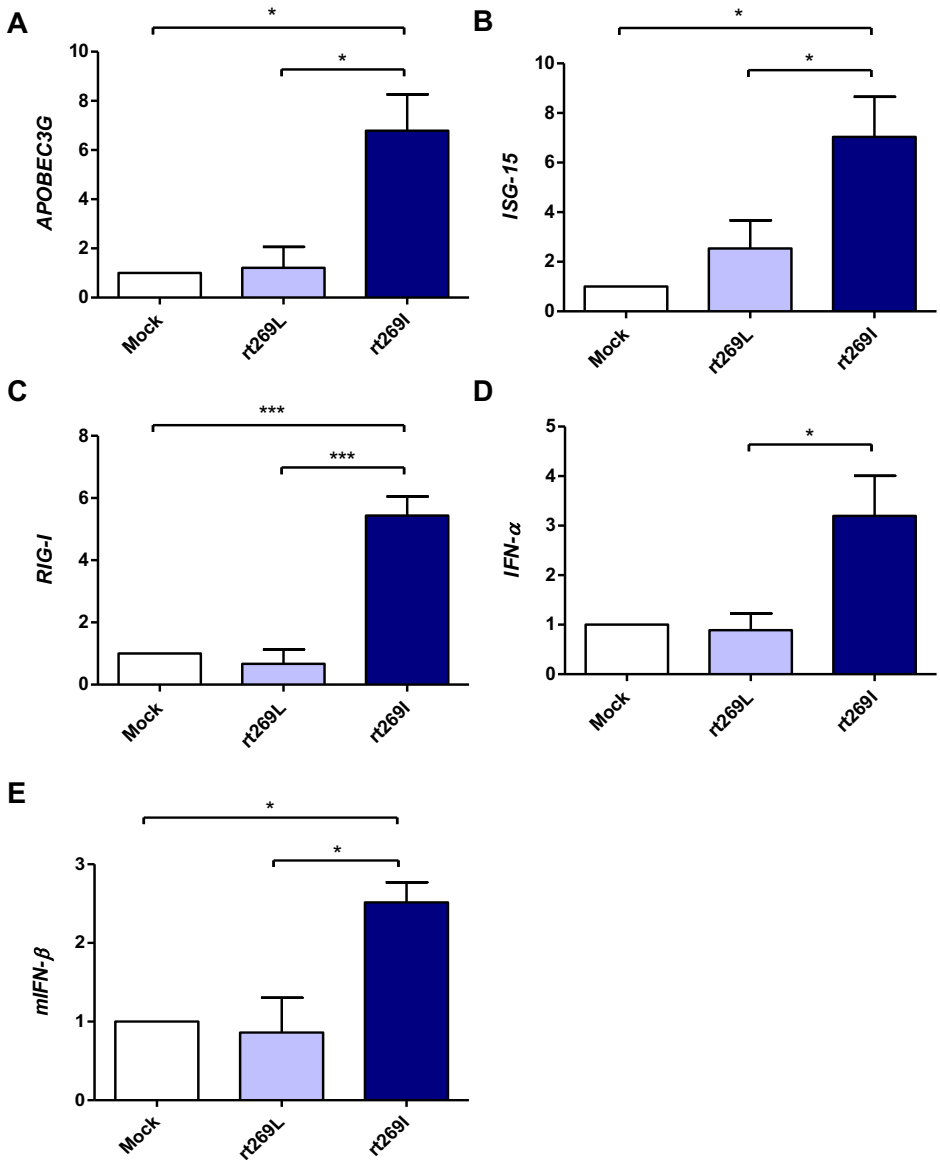
A
APOBEC3G
10
8
6
4
2
0
*
*
Mock
rt269L
rt269I
B
ISG-15
10
8
6
4
2
0
*
*
Mock
rt269L
rt269I
C
RIG-I
8
6
4
2
0
***
***
Mock
rt269L
rt269I
D
IFN-α
5
4
3
2
1
0
*
Mock
rt269L
rt269I
E
mIFN-β
3
2
1
0
*
*
Mock
rt269L
rt269I

Figure 5. rt269I enhanced IFN-I production *in vivo* assay. Both HBV-encoding DNA and pSV-β-Galactosidase were injected by hydrodynamic tail vein injection into C57BL/6 mice (*n*=5). The transcription level of APOBEC3G **(A)**, ISG-15 **(B)**, RIG-I **(C)**, IFN-α **(D)**, and IFN-β **(E)** were determined by qRT-PCR from mice hepatocytes on 4 days post-infection, and normalized with 18S rRNA and *β-Galactosidase*. Data represent mean±S.D. One-way ANOVA were used. $^{*}p<0.05$, $^{**}p<0.01$, $^{***}p<0.001$.

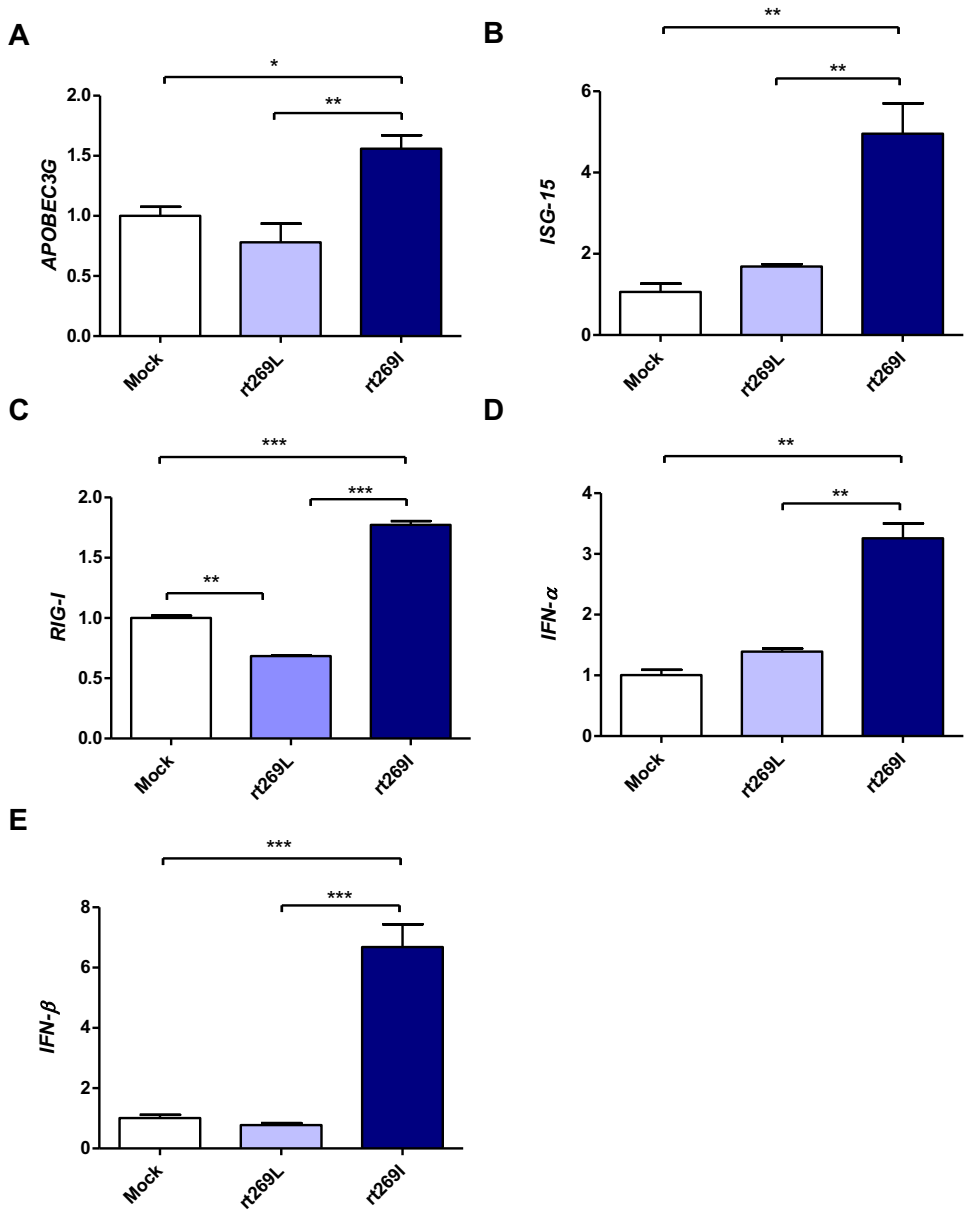
A
APOBEC3G
2.0
1.5
1.0
0.5
0.0
*
**
Mock
rt269L
rt269I
B
ISG-15
6
4
2
0
**
**
Mock
rt269L
rt269I
C
RIG-I
2.0
1.5
1.0
0.5
0.0
***
***
**
Mock
rt269L
rt269I
D
IFN-α
4
3
2
1
0
**
**
Mock
rt269L
rt269I
E
IFN-β
8
6
4
2
0
***
***
Mock
rt269L
rt269I

Figure 6. Hepatocytes increased transcription level of IFN-I against rt269I infection. HepG2 cells were co-transfected with HBV DNA and pSV-β-Galactosidase, and the expression levels of IFN-I-related genes, APOBEC3G **(A)**, ISG-15 **(B)**, RIG-I **(C)**, IFN-α **(D)**, and IFN-β **(E)**, were assessed. The mRNA level of IFN-I-related genes was determined using qRT-PCR at 12 hours after transfection, and data were normalized to 18S rRNA. Data represent mean±S.D. One-way ANOVA were used. $^{*}p<0.05$, $^{**}p<0.01$, $^{***}p<0.001$.

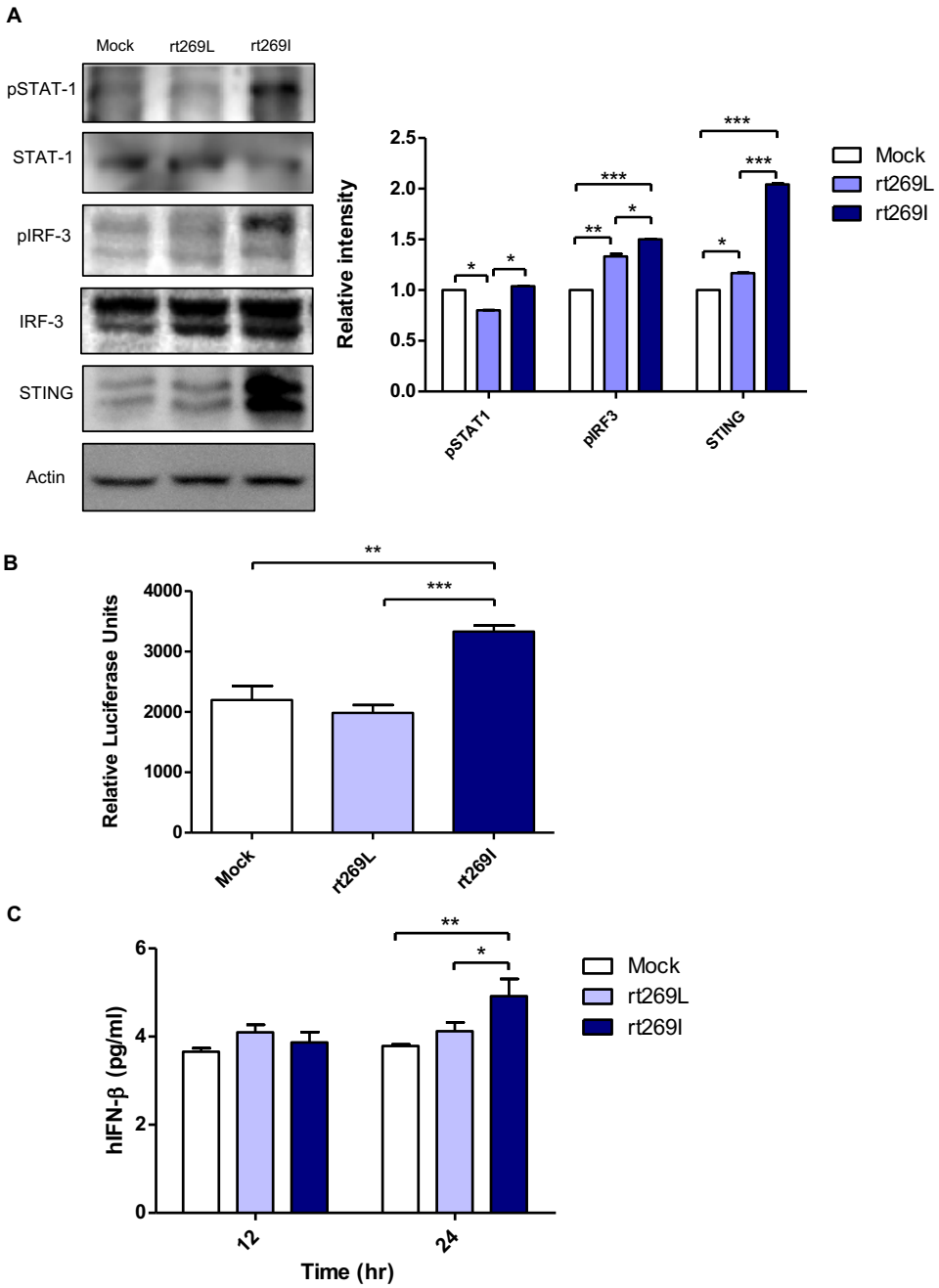
A
Mock
rt269L
rt269I
pSTAT-1
STAT-1
pIRF-3
IRF-3
STING
Actin
Relative intensity
2.5
2.0
1.5
1.0
0.5
0.0
pSTAT1
pIRF3
STING
Mock
rt269L
rt269I
B
Relative Luciferase Units
4000
3000
2000
1000
0
Mock
rt269L
rt269I
C
hIFN-β (pg/ml)
6
4
2
0
12
24
Time (hr)
Mock
rt269L
rt269I

Figure 7. HepG2 cells activated IFN-I signaling pathway and produced INF-I against rt269I. pHBV-1.2x-rt269L and -rt269I were co-transfected with pSV-β-Galactosidase into HepG2 cells. **(A)** The upstream proteins of the IFN-I signaling pathway were detected via Western blotting at 48 hours post-transfection. **(B)** The culture supernatant was collected at 24 hours post-transfection and used to measure IFN-I using a luciferase assay with HEK293 cells with the construct of the luciferase reporter gene under the control of IRSE promoter. **(C)** The secreted IFN-β was measured with ELISA at 24 hours post-transfection. Data were and normalized to β-Galactosidase assay. One- and two-way ANOVA were used. $^{*}p<0.05$, $^{**}p<0.01$, $^{***}p<0.001$.

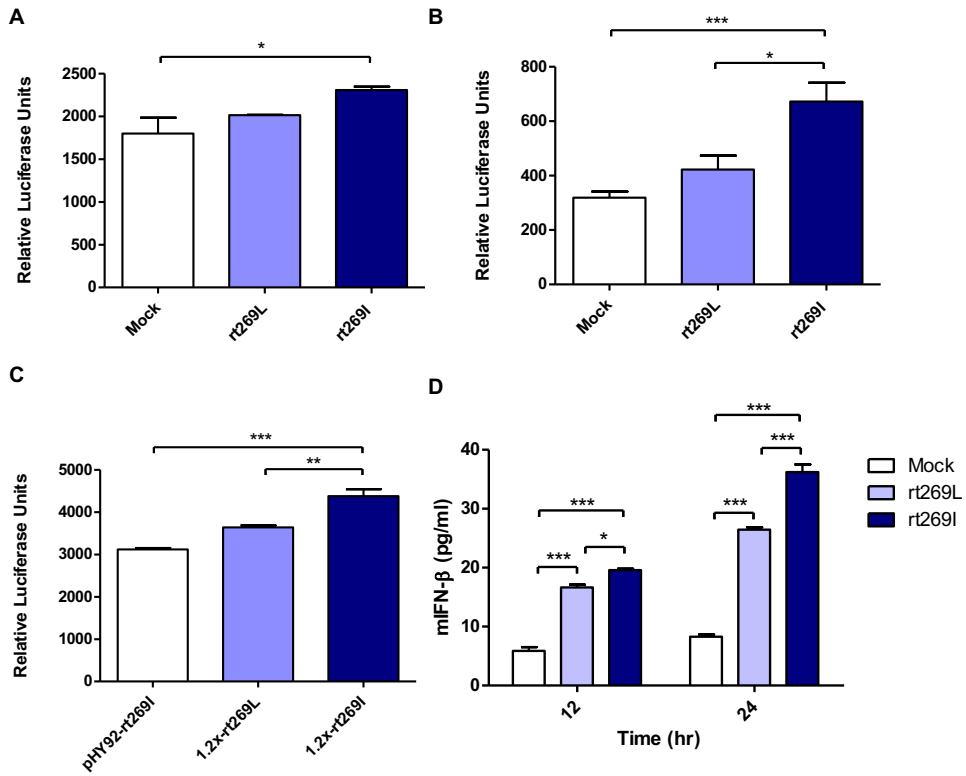

Figure 8. IFN-I production was enhanced in hepatocytes infected with rt269I. **(A-C)** The culture supernatant was collected at 24 hours post-transfection and used to measure IFN-I. pHBV-1.2x-mock, rt269L, and rt269I plasmid DNA (genotype C) were transfected into the Huh 7 **(A)** and Huh 7.5 cells **(B)**. **(C)** pHY92-1.1x-HBV-rt269I (genotype A), 1.2x-rt269L (genotype C), and 1.2x-rt269I (genotype C) plasmid DNA were transfected into the HepG2 cells and the IFN-I levels were compared among the groups. (**D)** HBV DNA were transfected into mouse hepatoma cell Hepa1c1c-7, and mouse IFN- β in the supernatants were measured by ELISA. These data were normalized with β-Galactosidase assay. Data represent mean±S.D. One- and two-way ANOVA were used. $^{*}p<0.05$, $^{**}p<0.01$, $^{***}p<0.001$.

5. The reduced replication capacity and enhanced IFN-I expression of rt269I were also proved in two HBV infection models.

To determine whether the different replication capacity between rt269L and rt269I could be reproduced in HBV virion infection assays, HepaRG and HepG2-hNTCP-C4 which have been widely used for the HBV infection models were used [53, 54]. In HepG2-hNTCP-C4 cells, intracellular HBV DNA level was also significantly increased in rt269L HBV infected cells compared with that of rt269I HBV infected cells on day 3 (**Figure 9A**). In addition, rt269I-HBV-infected HepG2-hNTCP-C4 cells showed lower cccDNA level compared with rt269L-HBV-infected cells on day 5 **(Figure 9B)**. Futhermore, the secreted HBsAg was more elevated in rt269L infected group than rt269I and this pattern was maintained until day 5 after infection (**Figure 9C**). Consistently, extracellular HBV DNA level was also increased in rt269L HBV infected cells compared with that of rt269I HBV infected cells on day 3 (**Figure 9D)**. The different replication capacities from infection between rt269L and rt269I HBV were further verified in HepaRG cells. Intracellular HBV DNA level was greatly increased in rt269L versus rt269I HBV infected group, and the most distinct difference between two groups was shown on day 2 **(Figure 9E)**. Reduced cccDNA level, shown in rt269I-HBV infected HepG2-hNTCP-C4 cells, was also reproduced in HepaRG cells on day 3 (**Figure 9F**). Furthermore, IFN-I secretion levels were measured by an ISRE promoter-luciferase assay. As shown in transient transfection system, rt269I-infected-HepG2-hNTCP-C4 cells and –HepaRG cells secreted larger amount of IFN-I compared with rt269L-infected cells

on Day 5 and day 0, respectively (**Figure 9G** and **H)**. Together, I also proved that rt269I leads to reduced HBV replication and enhanced IFN-I production in HBV virion infection model system, compared to rt269L.

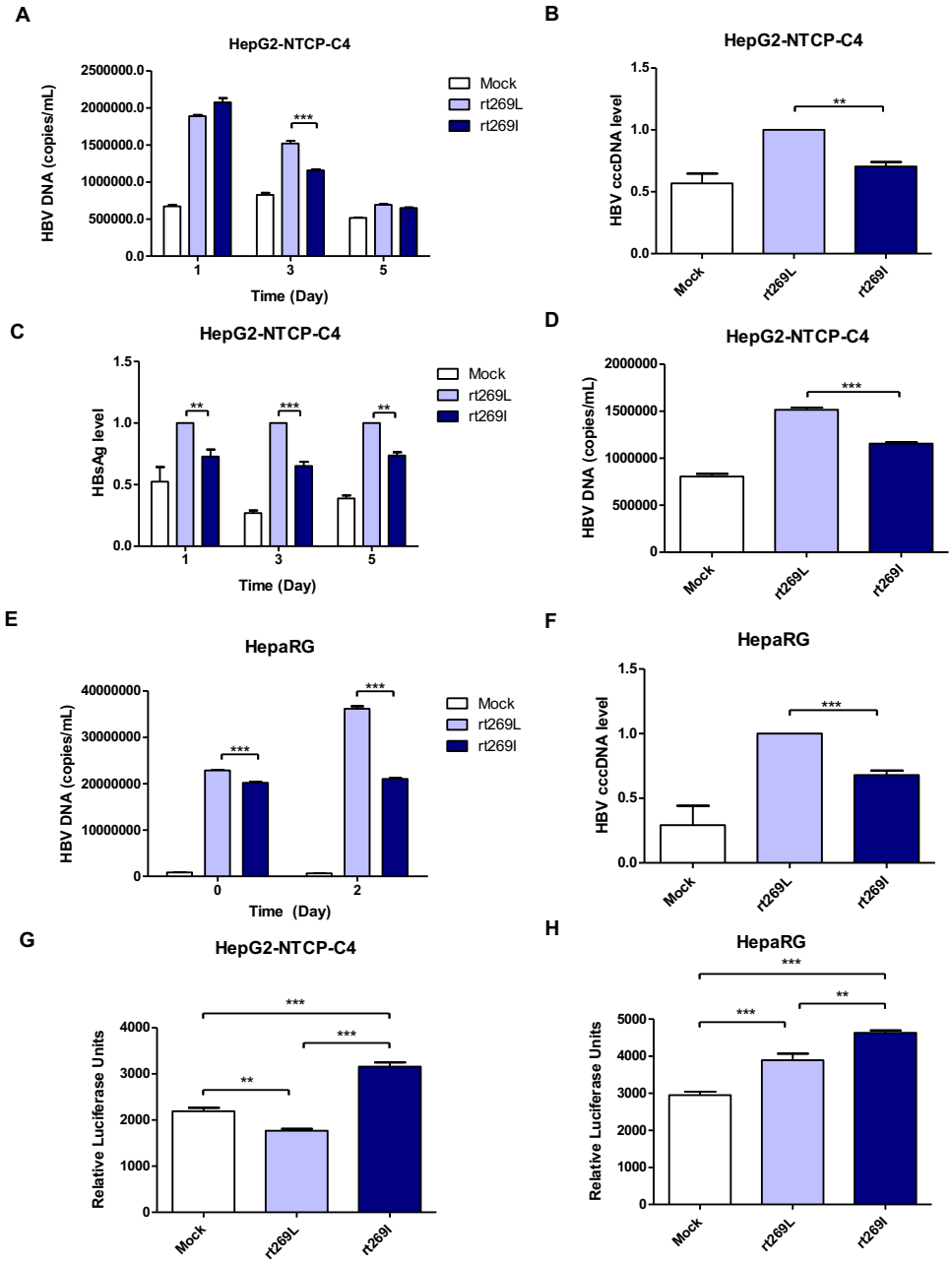
A
HepG2-NTCP-C4
HBV DNA (copies/mL)
2500000.0
2000000.0
1500000.0
1000000.0
500000.0
0.0
1
3
5
Time (Day)
Mock
rt269L
rt269I
***
B
HepG2-NTCP-C4
HBV cccDNA level
1.5
1.0
0.5
0.0
**
Mock
rt269L
rt269I
C
HepG2-NTCP-C4
HBsAg level
1.5
1.0
0.5
0.0
**
***
**
1
3
5
Time (Day)
Mock
rt269L
rt269I
D
HepG2-NTCP-C4
HBV DNA (copies/mL)
2000000
1500000
1000000
500000
0
***
Mock
rt269L
rt269I
E
HepaRG
HBV DNA (copies/mL)
40000000
30000000
20000000
10000000
0
***
***
0
2
Time (Day)
Mock
rt269L
rt269I
F
HepaRG
HBV cccDNA level
1.5
1.0
0.5
0.0
***
Mock
rt269L
rt269I
G
HepG2-NTCP-C4
Relative Luciferase Units
4000
3000
2000
1000
0
***
**
***
Mock
rt269L
rt269I
H
HepaRG
Relative Luciferase Units
5000
4000
3000
2000
1000
0
***
***
**
Mock
rt269L
rt269I

Figure 9. The reduced replication capacity of rt269I was shown in HBV infection models. (**A-D**) rt269L- or rt269I- HBV variant infection of HepG2-hNTCP-C4 cells. (**A**) Intracellular HBV DNA level were evaluated using qPCR on day 1, 3, and 5. **(B)** HBV cccDNA level was measured in HepG2-hNTCP-C4 cells infected by each HBV variant on day 5. (**C**) HBsAg secretion in the supernatant of infected cells were measured using ELISA on day 1, 3, and 5. (**D**) Extracellular HBV DNA level were evaluated using qPCR on day 3. (**E and F**) rt269L- or rt269I-HBV variant infection of HepaRG cells. (**E**) Intracellular HBV DNA level was measured using qPCR on day 0 and 2. (**F**) HBV cccDNA level was evaluated in HepaRG cells infected by each HBV variant on day3. (**G and H**) The secreted IFN-I in HepG2-hNTCP-C4 (**G**) and HepaRG cells (**H**) infected by each construct was measured using luciferase reporter assay on Day 5 and day 0, respectively. Data represents mean ± S.D. of three independent experiments. One- and two-way ANOVA were used. $^{*}p<0.05$, $^{**}p<0.01$, $^{***}p<0.001$.

6. The replication of rt269I was inhibited via STING- IFN-I axis.

Since the secretion of IFN-I exerts antiviral effects against HBV [55, 56], the above finding showed that IFN-I was produced in the cells transfected rt269I. Therefore, I checked whether replication inhibition found in rt269I depends on IFN-I signaling. I found that the decreased HBsAg and HBeAg level in rt269I were neutralized or even reversed when the IFN-I signal was blocked via IFNAR2 neutralization at 48 hours post-transfection (**Figure 10A**). To further check IFN-I signal dependence of rt269I replication, JAK-STAT pathway was inhibited using AZD1480. As shown in IFNAR2 neutralization, the inhibition of HBsAg and HBeAg level in rt269I was reversed by inhibition of JAK-STAT pathway at 48 hours after transfection (**Figure 10B**). Furthermore, I found that the siRNA mediated knockdown of STING, but not scramble could lead to reversion of inhibition on HBV replication or HBsAg secretion as found in the rt269I type at 48 hours post-transfection (**Figure 10C**). Together, these results indicated that rt269I leads lower levels of HBV replication via STING- IFN-I-axis in hepatocytes.

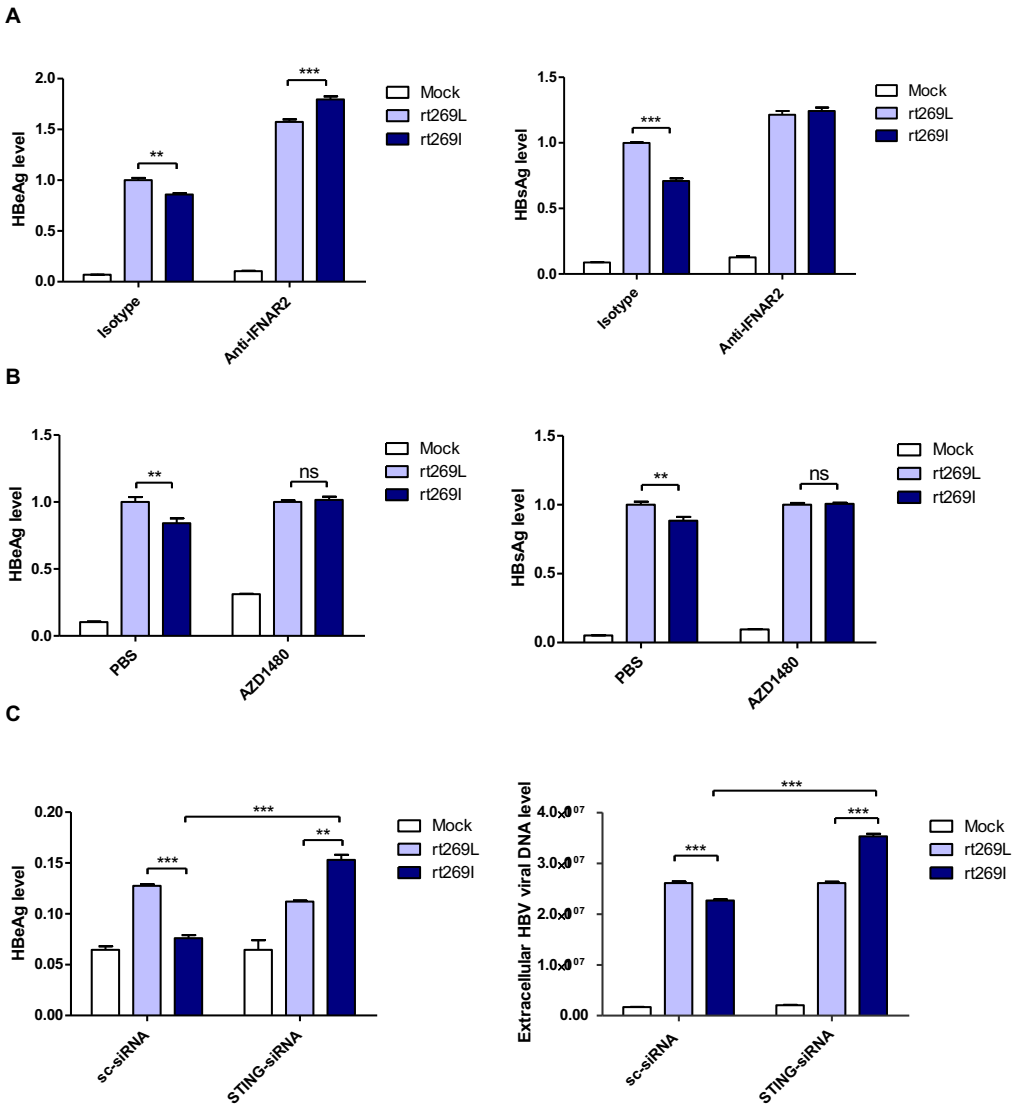
A
HBeAg level
2.0
1.5
1.0
0.5
0.0
**
***
Isotype
Anti-IFNAR2
Mock
rt269L
rt269I
HBsAg level
1.5
1.0
0.5
0.0
***
Isotype
Anti-IFNAR2
Mock
rt269L
rt269I
B
HBeAg level
1.5
1.0
0.5
0.0
**
ns
PBS
AZD1480
Mock
rt269L
rt269I
HBsAg level
1.5
1.0
0.5
0.0
**
ns
PBS
AZD1480
Mock
rt269L
rt269I
C
HBeAg level
0.20
0.15
0.10
0.05
0.00
***
***
**
sc-siRNA
STING-siRNA
Mock
rt269L
rt269I
Extracellular HBV viral DNA level
4.0x10^07
3.0x10^07
2.0x10^07
1.0x10^07
0.00
***
***
***
sc-siRNA
STING-siRNA
Mock
rt269L
rt269I

Figure 10. The replication inhibition found in rt269I was mediated via STING-IFN-I axis. (**A**) IFNAR2 was blocked using anti-IFNAR2 antibody (10 μg) and HBV-encoding DNA and pSV-β-Galactosidase were transiently transfected into HepG2 cells. HBsAg and HBeAg in the presence of isotype or anti-IFNAR2 antibody were measured using ELISA at 48 hours post-transfection. (**B**) HepG2 cells pre-treated with AZD1480 (5 μM) for 2 hours were transfected with HBV DNA pSV-β-Galactosidase and constantly treated with AZD1480. HBsAg and HBeAg were measured using ELISA at 48 hours post-transfection. (**C**) HBV DNA constructs and pSV-β-Galactosidase were co-transfected with either STING or scramble siRNA into HepG2 cells. The HBeAg levels and HBV virions were analyzed using ELISA and qPCR, respectively at 48 hours post-transfection. Data were normalized with β-Galactosidase enzyme assay, and represents mean ± S.D. of three independent experiments. One- and two-way ANOVA were used. $^{*}p<0.05$, $^{**}p<0.01$, $^{***}p<0.001$.

7. rt269I enhanced mitochondrial stress mediated IFN-I production and heme oxygenase (HO)-1.

As bilirubin is one of the final byproducts of inducible HO-1 [57], the clinical data showing higher levels of bilirubin in serum of patients with rt269I (**Table 1**) also suggest that rt269I could enhance HO-1 expression. As expected, the expressed HO-1 significantly increased in the transcription and translation levels in cells with rt269I (**Figure 11A** and **B**). Previously, HO-1 has been reported to be induced by mitochondrial stress or ROS [58]. Thus, I assessed whether mitochondrial ROS (mtROS) could be enhanced in HepG2 cells infected with rt269I. Although both groups showed similar cytosolic ROS levels (data not shown), enhanced mtROS levels were found in cells with rt269I at 24 hours post-transfection (**Figure 12A and B**), suggesting that rt269I versus rt269L led to enhanced mitochondrial stress. To assess whether or not this effect is specific to genotype C, I compared mtROS production in HepG2 cells between two types of genotype C, rt269L and rt269I, and the wild type of genotype A with Pol of rt269I type via confocal analysis using MitoSox. Of these, genotype C-rt269I produced the strongest mtROS, suggesting that the enhancing trait of mtROS found in rt269I may also be specific to genotype C at 24 hours after transfection (**Figure 12C**). It has been reported that mtROS can cause oxidative mitochondrial DNA damage, resulting in increased mitochondrial 8-OHdG that is indicative of DNA damage [59]. I consistently observed that the quantification of 8-OHdG significantly increased in cells infected with rt269I at 48 hours post-transfection (**Figure 13A**). Next, I assessed if mtROS could act as

upstream signaling of enhanced IFN-I and HO-1 induction induced by rt269I via treatment of MitoTEMPO, a mitochondria-targeted antioxidant. The treatment of MitoTEMPO abrogated the increased IFN-I induced by rt269I at 24 hours post-transfection (**Figure 13B**). Furthermore, the elevated HO-1 mRNA levels induced by rt269I were also completely abrogated by MitoTEMPO treatment at 24 hours post-transfection (**Figure 13C**). Together, these results indicated that rt269I infections cause mitochondrial stress and the subsequent cytosol release of oxidized mtDNA, resulting in enhanced production of IFN-I and HO-1 in hepatocytes.

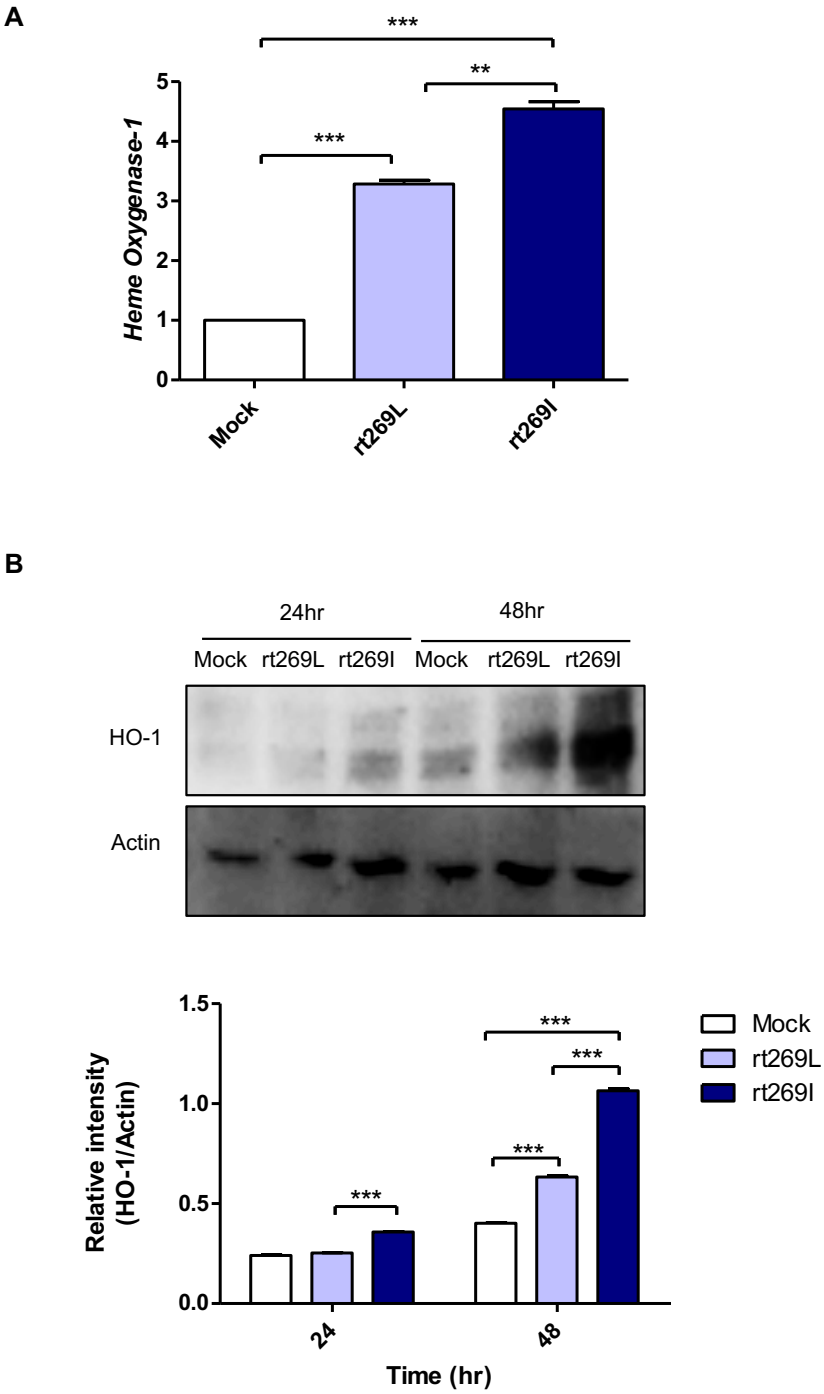
A
***
**
***
Heme Oxygenase-1
5
4
3
2
1
0
Mock
rt269L
rt269I
B
24hr
48hr
Mock rt269L rt269I Mock rt269L rt269I
HO-1
Actin
1.5
1.0
0.5
0.0
Relative intensity
(HO-1/Actin)
***
***
***
***
24
48
Time (hr)
Mock
rt269L
rt269I

Figure 11. HepG2 cells enhanced HO-1 in transcription and translation level against rt269I infection. HepG2 cells were transfected with HBV DNA and pSV-β-Galactosidase, and HO-1 production was assessed. **(A)** Transcription level of HO-1 was determined using qRT-PCR at 24 hours after transfection. **(B)** HO-1 protein was detected via Western blotting and actin was used as a control. Data were normalized by β-Galactosidase assay, and represent mean±SD of three independent experiments. $^{*}p<0.05$, $^{**}p<0.01$, and $^{***}p<0.001$.

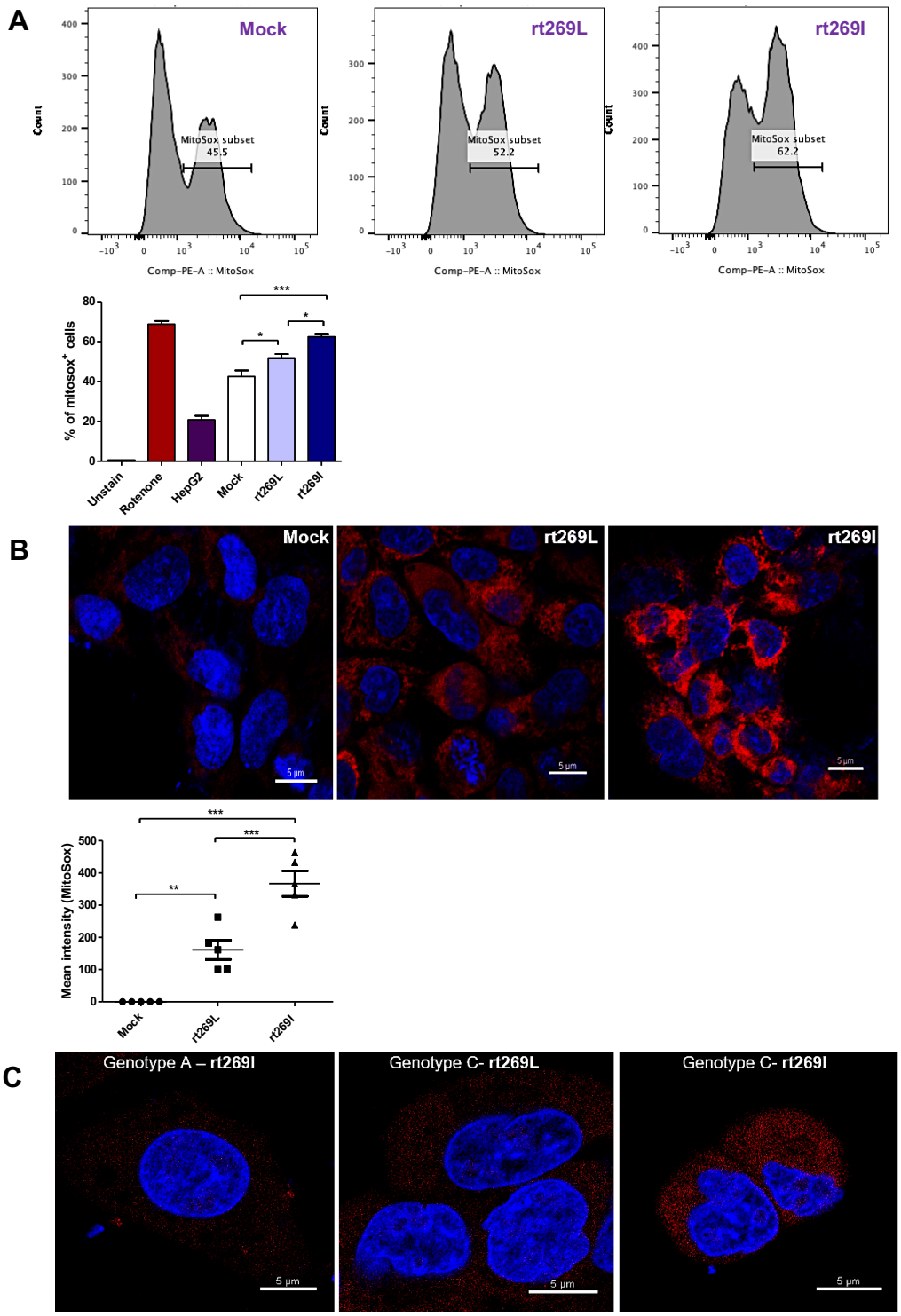
A
Mock
rt269L
rt269I
MitoSox subset
45.5
MitoSox subset
52.2
MitoSox subset
62.2
Count
Comp-PE-A :: MitoSox
% of mitosox+ cells
Unstain
Rotenone
HepG2
Mock
rt269L
rt269I
B
Mock
rt269L
rt269I
5 µm
Mean intensity (MitoSox)
C
Genotype A – rt269I
Genotype C- rt269L
Genotype C- rt269I

Figure 12. rt269I induced mitochondrial reactive oxygen species production. pHBV-1.2x-rt269L and -rt269I were co-transfected with pSV-β-Galactosidase into HepG2 cells, and mitochondrial stress was assessed. **(A and B)** Mitochondrial ROS was stained with MitoSOX (5 μM) and analyzed by flow cytometry **(A)** and confocal microscope **(B)**, followed by transfection for 24 hours. **(C)** The HepG2 cells were transfected with pHY92-rt269I (genotype A), 1.2x-rt269L (genotype C), and 1.2x-rt269I (genotype C) plasmid DNA. Data were normalized by β-Galactosidase assay, and represent mean±SD of three independent experiments. $^{*}p<0.05$, $^{**}p<0.01$, and $^{***}p<0.001$.

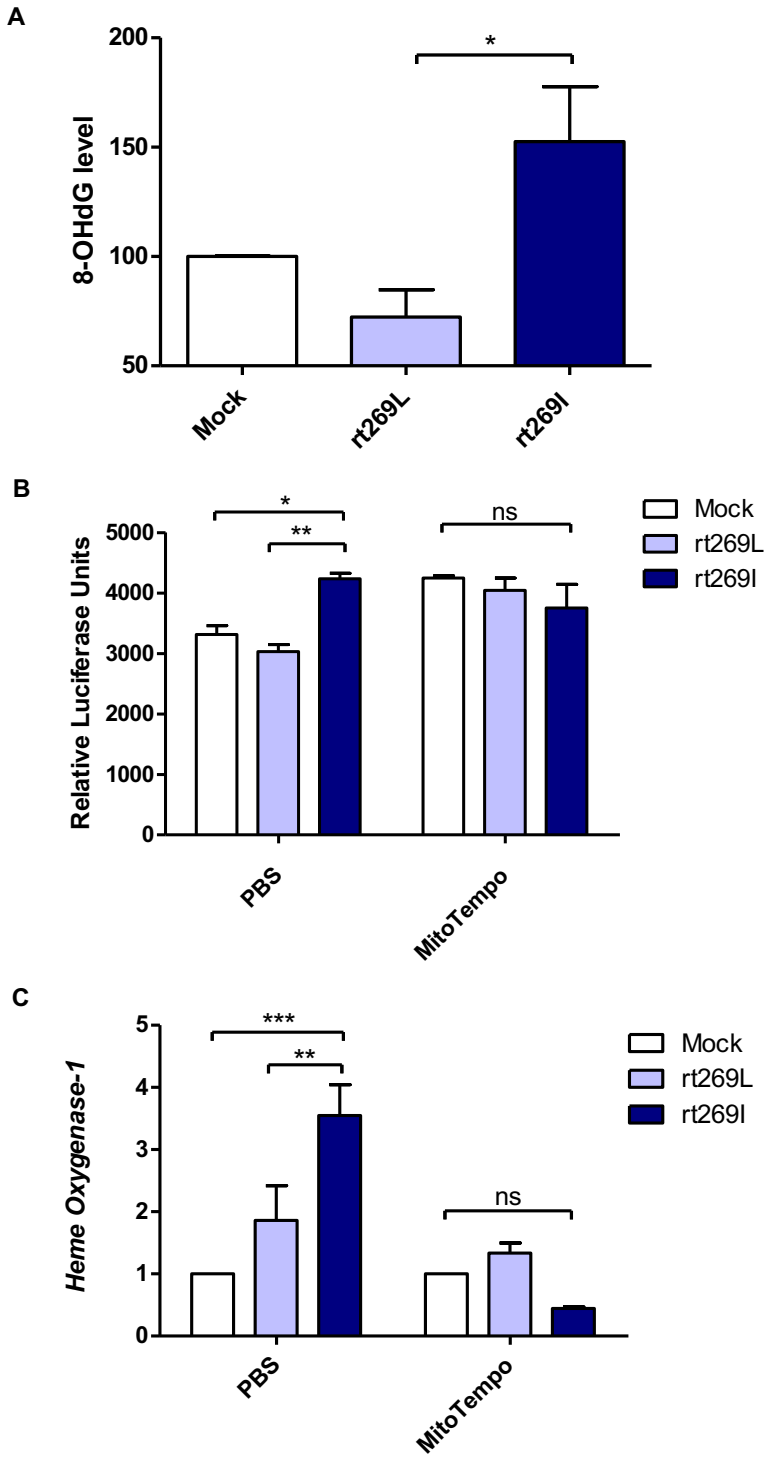
A
8-OHdG level
200
150
100
50
*
Mock
rt269L
rt269I
B
Relative Luciferase Units
5000
4000
3000
2000
1000
0
*
**
ns
Mock
rt269L
rt269I
PBS
MitoTempo
C
Heme Oxygenase-1
5
4
3
2
1
0
***
**
ns
Mock
rt269L
rt269I
PBS
MitoTempo

Figure 13. rt269I caused mitochondrial stress in infected hepatocytes. (A) HepG2 cells were co-transfected with HBV DNA and pSV-β-Galactosidase, and 8-OHdG was detected using ELISA. **(B and C)** MitoTEMPO (100 μM) was administrated to the transfcted cells. **(B)** IFN-I levels were assessed using an IRSE-luciferase assay at 24 hours after transfection. **(C)** qRT-PCR analysis of HO-1 mRNA levels were evaluated using qRT-PCR at 24 hours after transfection. Data represent mean±SD. of three independent experiments. $^{*}p<0.05$, $^{**}p<0.01$, and $^{***}p<0.001$.

8. rt269I enhanced iNOS dependent NO production.

It was previously reported that HBV infections could lead to nitric oxide (NO) mediated by inducible nitric oxide synthase (iNOS), which causes the inhibition of viral replication [60]. Thus, I assessed iNOS dependent NO production between rt269I and rt269L. In an *in vivo* mouse model, the transcription of iNOS was significantly enhanced in rt269I compared to rt269L on 3 days post-injection (**Figure 14A**). In *in vitro* systems of transfected HepG2 cells, rt269I led to enhanced iNOS expression via Western blotting at 48 hours post-transfection (**Figure 14B**). The secreted NO measured using ELISA was also significantly increased in rt269I at 24 hours post-transfection (**Figure 14C**). In addition, to better understand the antiviral effects of NO, the viral replication of both types was also assessed after treatment with iNOS inhibitor, N^{ω}-Nitro-L-arginine methyl ester hydrochloride (L-NAME). Treatment with L-NAME restored decreased HBsAg and HBeAg levels in both rt269I and rt269L types, but its effect was more pronounced in rt269I, suggesting that the lowered replication shown in rt269I may be in part due to its enhanced NO production at 24 hours post-transfection (**Figure 15A**). It has been reported that IFN-I can regulate iNOS dependent NO production as its upstream signal [24]. To further verify whether iNOS induction found in rt269I is dependent on IFN-I signaling, the iNOS expression levels of both types were analyzed from infected HepG2 cells after blocking IFNAR2. The increased transcription levels of iNOS found in rt269I were abrogated by blocking IFNAR2 at 24 hours post-transfection (**Figure 15B**). Together, the data indicated that rt269I could lead to enhanced iNOS dependent NO

production via IFN-I signaling, contributing to disease progression in chronic patients with genotype C infections.

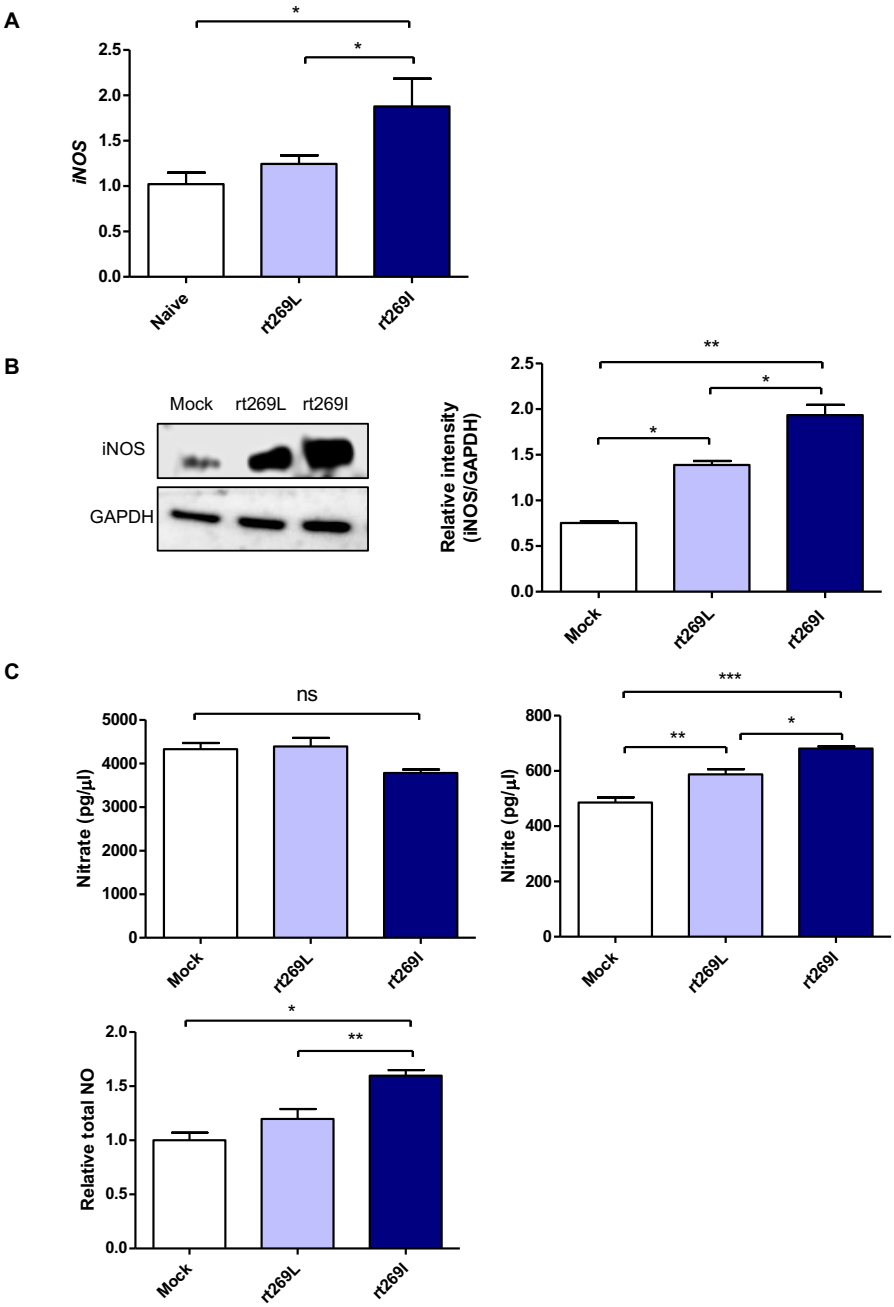
A
*
*
2.5
2.0
1.5
1.0
0.5
0.0
iNOS
Naive
rt269L
rt269I
B
Mock
rt269L
rt269I
iNOS
GAPDH
**
*
*
2.5
2.0
1.5
1.0
0.5
0.0
Relative intensity (iNOS/GAPDH)
Mock
rt269L
rt269I
C
ns
5000
4000
3000
2000
1000
0
Nitrate (pg/μl)
Mock
rt269L
rt269I
***
**
*
800
600
400
200
0
Nitrite (pg/μl)
Mock
rt269L
rt269I
*
**
2.0
1.5
1.0
0.5
0.0
Relative total NO
Mock
rt269L
rt269I

Figure 14. rt269I enhanced iNOS dependent NO production. (A) The HBV constructs were injected with hydrodynamic tail vein into C57BL/6 mice (*n*=5). Transcription levels of iNOS in hepatocytes were determined using qPCR and were normalized with 18S rRNA on 3 days post-injection. **(B and C)** HepG2 cells were transfected with HBV construct and pSV-β-Galactosidase was co-transfected to normalization. **(B)** iNOS synthesis was detected via Western blot analysis at 48 hours after transfection. **(C)** Poly(I:C) was co-transfected with HBV DNA and the secreted NO_2^- and NO_3^- were measured using ELISA at 24 hours post-transfection. One-way ANOVA were used. $^{*}p<0.05$; $^{**}p<0.01$; $^{***}p<0.001$; ns, not significant.

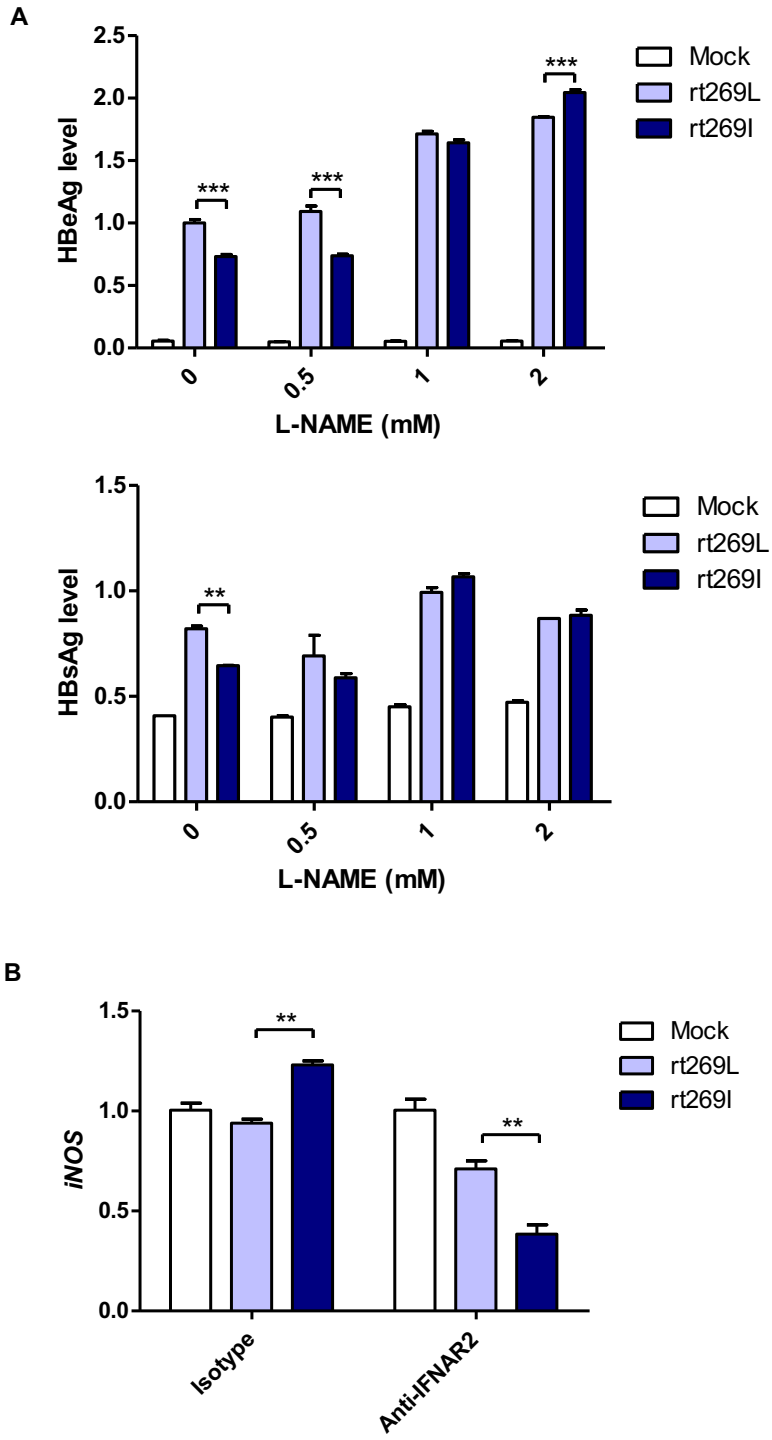
A
HBeAg level
2.5
2.0
1.5
1.0
0.5
0.0
***
***
***
0
0.5
1
2
L-NAME (mM)
Mock
rt269L
rt269I
HBsAg level
1.5
1.0
0.5
0.0
**
0
0.5
1
2
L-NAME (mM)
Mock
rt269L
rt269I
B
iNOS
1.5
1.0
0.5
0.0
**
**
Isotype
Anti-IFNAR2
Mock
rt269L
rt269I

Figure 15. rt269I enhanced iNOS dependent NO production in IFN-I dependent manner. (A) HepG2 cells pre-treated with L-NAME for 2 hours were transfected with HBV DNA and constantly treated with L-NAME. The secreted HBsAg and HBeAg were detected by ELISA at 24 hours. **(B)** IFN-I signaling was blocked by anti-IFNAR2 antibody (5 μg) for 12 hours and iNOS gene expression was determined using qRT-PCR at 24 hours after transfection. Data are shown as mean±SD. One- and two-way ANOVA were used. $^{*}p<0.05$; $^{**}p<0.01$; $^{***}p<0.001$; ns, not significant.

DISCUSSION

Of 10 different HBV genotypes, genotype C and genotype B are responsible for the majority of HBV infections in endemic Asian countries [40]. In particular, it has been reported that most HBV infections in South Korea are due to genotype C [61], which may be a major reason for the lower response of IFN therapy [62] or NA therapy [63], the higher level of disease progression [64], and the higher prevalence of occult infection via vertical transmission [65, 66], observed in Korean CHB patients compared to patients in other areas. The current study investigated the virological or clinical factors and modulating capacity of antiviral IFN-I innate immunity between rt269L and rt269I in HBV genotype C infections. There are some noteworthy findings.

The clinical data using a Korean cohort proved that rt269L and rt269I showed distinct clinical or virological traits in HBV replication, HBsAg production, HBeAg serostatus, and biliverdin production (**Table 1**). This strongly suggests that there may be differences in modulating antiviral IFN-I production between rt269L and rt269I. Given a previous report indicating that the better response of genotype B than that of genotype C infections in IFN-α therapy was attributed to a higher level of HBeAg seroconversion via IFN-α mediated preC mutations [67], rt269I versus rt269L, more related to lower HBV replication or the HBsAg level and more related to HBeAg negative serostatus was expected to lead to enhanced IFN-I production.

Furthermore, a higher level of bilirubin, which is one of the final products of IFN-I mediated HO-1 metabolism, was also found in patients with rt269I type, further supporting the aforementioned findings.

The further epidemiologic data showed that HBeAg seronegative status observed in patients with rt269I was due to a higher frequency of preC mutations (G to A at 1896) induced via IFN-I mediated APOBEC3G (**Table 4** and **Figure 6**). This suggests that longer durations of HBeAg positive stages and lower levels of preC mutation frequency observed in patients with genotype C than that of genotype B infections [40] may be due to the presence of rt269L only in patients with genotype C. Actually, the further mechanism study showed that rt269L could produce lower levels of IFN-I production than rt269I, leading to a lower expression of ISGs including APOBEC3G in *in vitro* and *in vivo* systems, further supporting the epidemiological findings. The epidemiologic data also showed that rt269L (63%) was more prevalent than rt269I (37%) in the Korean cohort, unlike other areas showing more prevalence of rt269I versus rt269L (rt269I vs rt269L: 57% versus 43%). This suggests that rt269L showed not only high replication factors such as HBeAg, HBsAg, and HBV DNA level but also low preC mutation frequencies. These features of rt269L can be indicated with characteristics of genotype C, which was not shown in other genotypes. In addition, I suggest it may have a merit in infections into hosts via perinatal or vertical routes, contributing to chronic infections as a major type in South Korea. It is tempting to speculate that the higher prevalence of rt269L may contribute to some unique clinical traits found in South Korean CHB

patients, including the frequent failure of IFN-α therapy or NA treatments [62, 63] and the higher prevalence of occult HBV infections via vertical routes [65, 66]. However, this issue demands further investigation in the future.

The mechanism study indicated that distinct IFN-I production between rt269L and rt269I was attributed to different induction capacity of mitochondrial stress (**Figure 12**). Thus, rt269I versus rt269L can lead to enhanced production of mtROS and oxidized mtDNA, resulting in induced IFN-I production via cytosolic DNA sensing through the STING-IRF3 dependent pathway. To date, distinct capacity of mitochondrial stress induced by HBV genotypes, polymorphisms, or mutations has not been elucidated. HBV Pol was recently reported to interfere with antiviral IFN-I production through DNA sensing via the inhibition of STING polyubiquitination [36]. Thus, the functional difference in Pol due to SNP could contribute to differences in the two types of mitochondrial stress mediated IFN-I production. However, the molecular details regarding this issue remain to be elucidated in the future.

I found enhanced HO-1 expression and iNOS dependent NO production as a downstream pathway of IFN-I in rt269I. The enhanced HO-1 expression in rt269I exerted anti-HBV effects via the inhibition of virion capsid formation, in line with previous reports showing the anti-HBV effects of HO-1 [68]. It has also been reported that iNOS dependent NO production as another downstream pathway of INF-I could play a pivotal role in inflammatory responses and disease progression in the liver, including fibrosis and cirrhosis [24]. I also found enhanced production

of iNOS and NO in HepG2 cells transfected with rt269I (**Figure 14**), in line with the clinical data showing that patients with rt269I type infections were more related to disease progression. Enhanced iNOS and NO could also increase the frequency of preC mutations shown in rt269I, leading to HBeAg negative infections in chronic patients. The iNOS dependent NO production and mtROS production can synergistically exert apoptotic cell death in the liver, also facilitating the progression of liver diseases [69], further supporting the hypothesis regarding the contribution of rt269I to disease progression. (**Figure 16**).

The finding showing rt269L versus rt269I type led to enhanced HBV replication via inhibiting IFN-I production via STING-IFN-I axis is contrast to that reported by Ahn et al [70], previously. Maybe, the difference between two studies may be due to use of HBV genome plasmid from different patients with distinct genome sequences or difference of used cell lines. The pHBV-1.2x (GenBank accession No. AY641558) plasmid construct used in this study has no special mutations affecting HBV virology and virulence and have been widely used for genotype C mutation analysis and virulence studies [49, 71-73]. Furthermore, together the HBV genome transient study into diverse human hepatocytes and mouse hepatoma cell lines, the *in vivo* hydrodynamic injection study, in vitro HBV virion infection study and even the clinical data consistently supported enhanced HBV replication of rt269L versus rt269I type.

In conclusion, the data showed that rt269I could contribute to HBeAg negative infections and liver disease progression in CHB patients with genotype C

infections via mitochondrial stress mediated IFN-I production. In addition, enhanced iNOS dependent NO production induced by rt269I could also provide an additive role in disease progression. Furthermore, the finding could also provide likely explanation into characteristic features of genotype C with higher frequency of rt269L type, including longer durations of HBeAg positive stages and higher infectivity (**Figure 16**).

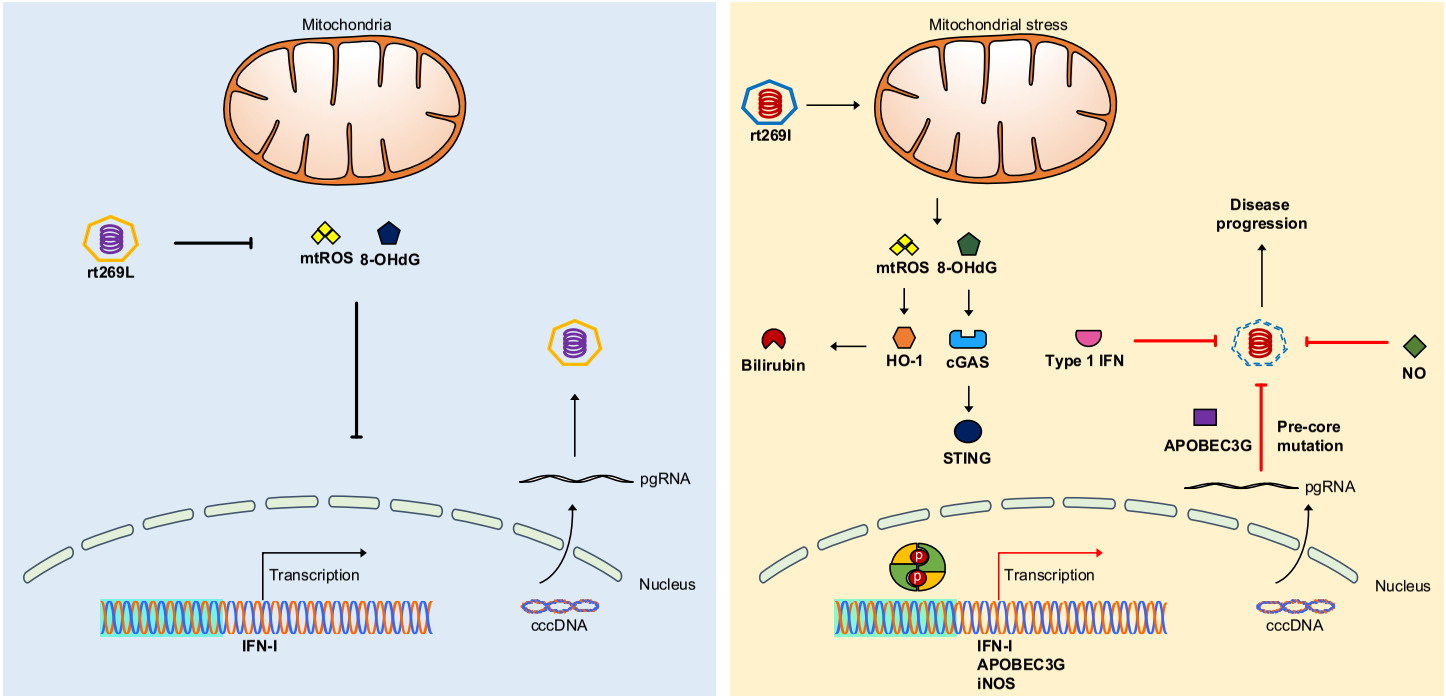
Mitochondria
rt269L
mtROS
8-OHdG
pgRNA
Transcription
Nucleus
cccDNA
IFN-I
Mitochondrial stress
rt269I
mtROS
8-OHdG
Disease progression
Bilirubin
HO-1
cGAS
Type 1 IFN
NO
STING
APOBEC3G
Pre-core mutation
pgRNA
Transcription
Nucleus
cccDNA
IFN-I
APOBEC3G
iNOS

Figure 16. Schematic presentation indicating distinct mitochondrial stress mediated IFN-I production and its distinct contribution to disease progression in chronic patients with genotype C infections between rt269L and rt269I. In contrast to rt269L, rt269I infection in genotype C induced mitochondrial ROS production, which led to an increased release of oxidized DNA into the cytosols of the infected hepatocytes. Sensing the oxidized DNA exposed to cytosol via the cGAS-STING pathway could lead to IFN-I production. Enhanced INF-I production in rt269I could exert several biological activities. First, it can lead to the increased inhibition of HBV replication via the inhibition of capsid formation by HO-1 production. Second, IFN-I mediated enhanced expression of APOBEC3G and iNOS can lead to HBeAg negative infection and liver disease progression via frequent generation of preC mutations at 1896 (G to A). Thus, rt269L can contribute to HBeAg negative infection and disease progression in chronic patients infected with genotype C via mitochondrial stress mediated enhanced INF-I production.

REFERENCES

1. Perz, J.F., et al., *The contributions of hepatitis B virus and hepatitis C virus infections to cirrhosis and primary liver cancer worldwide.* J Hepatol, 2006. **45**(4): p. 529-38.
2. Mortality, G.B.D. and C. Causes of Death, *Global, regional, and national life expectancy, all-cause mortality, and cause-specific mortality for 249 causes of death, 1980-2015: a systematic analysis for the Global Burden of Disease Study 2015.* Lancet, 2016. **388**(10053): p. 1459-1544.
3. Nannini, P. and E.M. Sokal, *Hepatitis B: changing epidemiology and interventions.* Archives of Disease in Childhood, 2017. **102**(7): p. 676-680.
4. Kwak, H.W., et al., *Clinical outcomes of a cohort series of patients with hepatocellular carcinoma in a hepatitis B virus-endemic area.* J Gastroenterol Hepatol, 2014. **29**(4): p. 820-9.
5. MacLachlan, J.H. and B.C. Cowie, *Hepatitis B Virus Epidemiology.* Cold Spring Harbor Perspectives in Medicine, 2015. **5**(5).
6. Sonigo, P. and P. Tiollais, *The Hepatitis-B Virus.* Bulletin De L Institut Pasteur, 1985. **83**(3): p. 181-206.
7. Yan, H., et al., *Sodium taurocholate cotransporting polypeptide is a functional receptor for human hepatitis B and D virus.* Elife, 2012. **1**.
8. Blondot, M.L., V. Bruss, and M. Kann, *Intracellular transport and egress of hepatitis B virus.* J Hepatol, 2016. **64**(1 Suppl): p. S49-S59.

9. Beck, J. and M. Nassal, *Hepatitis B virus replication.* World Journal of Gastroenterology, 2007. **13**(1): p. 48-64.

10. Lopatin, U., *Drugs in the Pipeline for HBV.* Clinics in Liver Disease, 2019. **23**(3): p. 535-+.

11. Werle-Lapostolle, B., et al., *Persistence of cccDNA during the natural history of chronic hepatitis B and decline during adefovir dipivoxil therapy.* Gastroenterology, 2004. **126**(7): p. 1750-1758.

12. Lucifora, J., et al., *Specific and Nonhepatotoxic Degradation of Nuclear Hepatitis B Virus cccDNA.* Science, 2014. **343**(6176): p. 1221-1228.

13. Ivanov, A.V., et al., *Oxidative stress, a trigger of hepatitis C and B virus-induced liver carcinogenesis.* Oncotarget, 2017. **8**(3): p. 3895-3932.

14. Guz, J., et al., *Comparison of Oxidative Stress/DNA Damage in Semen and Blood of Fertile and Infertile Men.* Plos One, 2013. **8**(7).

15. Cichoz-Lach, H. and A. Michalak, *Oxidative stress as a crucial factor in liver diseases.* World Journal of Gastroenterology, 2014. **20**(25): p. 8082-8091.

16. Kikuchi, G., T. Yoshida, and M. Noguchi, *Heme oxygenase and heme degradation.* Biochemical and Biophysical Research Communications, 2005. **338**(1): p. 558-567.

17. Espinoza, J.A., P.A. Gonzalez, and A.M. Kalergis, *Modulation of Antiviral Immunity by Heme Oxygenase-1.* American Journal of Pathology, 2017. **187**(3): p. 487-493.

18. Koliaraki, V. and G. Kollias, *A New Role for Myeloid HO-1 in the Innate to Adaptive Crosstalk and Immune Homeostasis.* Crossroads between Innate and Adaptive Immunity Iii, 2011. **780**: p. 101-111.

19. Honda, K., A. Takaoka, and T. Taniguchi, *Type I interferon gene induction by the interferon regulatory factor family of transcription factors (vol 25, pg 349, 2006).* Immunity, 2006. **25**(5): p. 849-849.

20. Kawai, T. and S. Akira, *The role of pattern-recognition receptors in innate immunity: update on Toll-like receptors.* Nature Immunology, 2010. **11**(5): p. 373-384.

21. Takeuchi, O. and S. Akira, *Pattern recognition receptors and inflammation.* Cell, 2010. **140**(6): p. 805-20.

22. Ivashkiv, L.B. and L.T. Donlin, *Regulation of type I interferon responses.* Nature Reviews Immunology, 2014. **14**(1): p. 36-49.

23. Schafer, S.L., et al., *Regulation of type I interferon gene expression by interferon regulatory factor-3.* Journal of Biological Chemistry, 1998. **273**(5): p. 2714-2720.

24. Bachmann, M., et al., *Type I interferon supports inducible nitric Oxide synthase in Murine hepatoma cells and hepatocytes and during experimental acetaminophen-induced liver Damage.* Frontiers in Immunology, 2017. **8**.

25. Sarkis, P.T., et al., *STAT1-independent cell type-specific regulation of antiviral APOBEC3G by IFN-alpha.* J Immunol, 2006. **177**(7): p. 4530-40.

26. Akaike, T. and H. Maeda, *Nitric oxide and virus infection.* Immunology, 2000. **101**(3): p. 300-8.

27. Stavrou, S. and S.R. Ross, *APOBEC3 Proteins in Viral Immunity.* J Immunol, 2015. **195**(10): p. 4565-70.

28. Xia, P.Y., et al., *DNA sensor cGAS-mediated immune recognition.* Protein & Cell, 2016. **7**(11): p. 777-791.

29. Shu, C., X. Li, and P.W. Li, *The mechanism of double-stranded DNA sensing through the cGAS-STING pathway.* Cytokine & Growth Factor Reviews, 2014. **25**(6): p. 641-648.

30. He, J., et al., *Inhibition of hepatitis B virus replication by activation of the cGAS-STING pathway.* Journal of General Virology, 2016. **97**: p. 3368-3378.

31. Sato, S., et al., *The RNA Sensor RIG-I Dually Functions as an Innate Sensor and Direct Antiviral Factor for Hepatitis B Virus.* Immunity, 2015. **42**(1): p. 123-132.

32. Christen, V., et al., *Inhibition of alpha interferon signaling by hepatitis B virus.* Journal of Virology, 2007. **81**(1): p. 159-165.

33. Faure-Dupuy, S., J. Lucifora, and D. Durantel, *Interplay between the Hepatitis B Virus and Innate Immunity: From an Understanding to the Development of Therapeutic Concepts.* Viruses-Basel, 2017. **9**(5).

34. Yu, S.Y., et al., *Hepatitis B virus polymerase inhibits RIG-I- and Toll-like receptor 3-mediated beta interferon induction in human hepatocytes through interference with interferon regulatory factor 3 activation and dampening of the interaction between TBK1/IKK epsilon and DDX3.* Journal of General Virology, 2010. **91**: p. 2080-2090.

35. Wang, X.M., et al., *Hepatitis B virus X protein suppresses virus-triggered IRF3 activation and IFN-beta induction by disrupting the VISA-associated complex.* Cellular & Molecular Immunology, 2010. **7**(5): p. 341-348.

36. Liu, Y.H., et al., *Hepatitis B Virus Polymerase Disrupts K63-Linked Ubiquitination of STING To Block Innate Cytosolic DNA-Sensing Pathways.* Journal of Virology, 2015. **89**(4): p. 2287-2300.

37. Kurbanov, F., Y. Tanaka, and M. Mizokami, *Geographical and genetic diversity of the human hepatitis B virus.* Hepatology Research, 2010. **40**(1): p. 14-30.

38. Lin, C.L. and J.H. Kao, *Hepatitis B Virus Genotypes and Variants.* Cold Spring Harbor Perspectives in Medicine, 2015. **5**(5).

39. Croagh, C.M.N., P.V. Desmond, and S.J. Bell, *Genotypes and viral variants in chronic hepatitis B: A review of epidemiology and clinical relevance.* World Journal of Hepatology, 2015. **7**(3): p. 289-303.

40. Sunbul, M., *Hepatitis B virus genotypes: global distribution and clinical importance.* World J Gastroenterol, 2014. **20**(18): p. 5427-34.

41. Lin, C.L. and J.H. Kao, *The clinical implications of hepatitis B virus genotype: Recent advances.* Journal of Gastroenterology and Hepatology, 2011. **26**: p. 123-130.

42. Chan, H.L.Y., et al., *Genotype C hepatitis B virus infection is associated with an increased risk of hepatocellular carcinoma.* Gut, 2004. **53**(10): p. 1494-1498.

43. Sunbul, M., *Hepatitis B virus genotypes: Global distribution and clinical importance.* World Journal of Gastroenterology, 2014. **20**(18): p. 5427-5434.

44. Kim, B.J., *Hepatitis B virus mutations related to liver disease progression of Korean patients.* World Journal of Gastroenterology, 2014. **20**(2): p. 460-467.

45. Kim, J.E., et al., *Naturally occurring mutations in the reverse transcriptase region of hepatitis B virus polymerase from treatment- naive Korean patients infected with genotype C2.* World Journal of Gastroenterology, 2017. **23**(23): p. 4222-4232.

46. Yoneyama, M., et al., *The RNA helicase RIG-I has an essential function in double-stranded RNA-induced innate antiviral responses.* Nature Immunology, 2004. **5**(7): p. 730-737.

47. Alexopoulou, A. and P. Karayiannis, *HBeAg negative variants and their role in the natural history of chronic hepatitis B virus infection.* World Journal of Gastroenterology, 2014. **20**(24): p. 7644-7652.

48. Zhang, D.K., et al., *Prevalent HBV point mutations and mutation combinations at BCP/preC region and their association with liver disease progression.* Bmc Infectious Diseases, 2010. **10**.

49. Kim, S.Y., et al., *An Effective Antiviral Approach Targeting Hepatitis B Virus with NJK14047, a Novel and Selective Biphenyl Amide p38 Mitogen-Activated Protein Kinase Inhibitor.* Antimicrobial Agents and Chemotherapy, 2017. **61**(8).

50. Noguchi, C., et al., *G to A hypermutation of hepatitis B virus.* Hepatology, 2005. **41**(3): p. 626-633.

51. Sato, M., et al., *Distinct and essential roles of transcription factors IRF-3 and IRF-7 in response to viruses for IFN-alpha/beta gene induction.* Immunity, 2000. **13**(4): p. 539-548.

52. Ma, F., et al., *Positive feedback regulation of type I interferon by the interferon-stimulated gene STING.* Embo Reports, 2015. **16**(2): p. 202-212.

53. Iwamoto, M., et al., *Evaluation and identification of hepatitis B virus entry inhibitors using HepG2 cells overexpressing a membrane transporter NTCP.* Biochemical and Biophysical Research Communications, 2014. **443**(3): p. 808-813.

54. Ni, Y. and S. Urban, *Hepatitis B Virus Infection of HepaRG Cells, HepaRG-hNTCP Cells, and Primary Human Hepatocytes.* Methods Mol Biol, 2017. **1540**: p. 15-25.

55. Belloni, L., et al., *IFN-alpha inhibits HBV transcription and replication in cell culture and in humanized mice by targeting the epigenetic regulation of the nuclear cccDNA minichromosome.* Journal of Clinical Investigation, 2012. **122**(2): p. 529-537.

56. Wieland, S.F., et al., *Interferon prevents formation of replication-competent hepatitis B virus RNA-containing nucleocapsids.* Proceedings of the National Academy of Sciences of the United States of America, 2005. **102**(28): p. 9913-9917.

57. Stocker, R., et al., *Bilirubin Is an Antioxidant of Possible Physiological Importance.* Science, 1987. **235**(4792): p. 1043-1046.

58. Abraham, N.G. and A. Kappas, *Pharmacological and clinical aspects of heme oxygenase.* Pharmacological Reviews, 2008. **60**(1): p. 79-127.

59. Valavanidis, A., T. Vlachogianni, and C. Fiotakis, *8-hydroxy-2' -deoxyguanosine (8-OHdG): A Critical Biomarker of Oxidative Stress and Carcinogenesis.*

Journal of Environmental Science and Health Part C-Environmental Carcinogenesis & Ecotoxicology Reviews, 2009. **27**(2): p. 120-139.

60. Guidotti, L.G., et al., *Nitric oxide inhibits hepatitis B virus replication in the livers of transgenic mice.* J Exp Med, 2000. **191**(7): p. 1247-52.

61. Kim, H., et al., *Molecular epidemiology of hepatitis B virus (HBV) genotypes and serotypes in patients with chronic HBV infection in Korea.* Intervirology, 2007. **50**(1): p. 52-57.

62. Kim, B.K., P.A. Revill, and S.H. Ahn, *HBV genotypes: relevance to natural history, pathogenesis and treatment of chronic hepatitis B.* Antiviral Therapy, 2011. **16**(8): p. 1169-1186.

63. Song, B.C., et al., *Hepatitis B e antigen seroconversion after lamivudine therapy is not durable in patients with chronic hepatitis B in Korea.* Hepatology, 2000. **32**(4): p. 803-806.

64. El-Serag, H.B., *Epidemiology of Viral Hepatitis and Hepatocellular Carcinoma.* Gastroenterology, 2012. **142**(6): p. 1264-+.

65. Kim, H., et al., *Naturally Occurring Mutations in Large Surface Genes Related to Occult Infection of Hepatitis B Virus Genotype C.* Plos One, 2013. **8**(1).

66. Kim, H. and B.J. Kim, *Association of preS/S Mutations with Occult Hepatitis B Virus (HBV) Infection in South Korea: Transmission Potential of Distinct Occult HBV Variants.* International Journal of Molecular Sciences, 2015. **16**(6): p. 13595-13609.

67. Yang, H.C., et al., *Distinct evolution and predictive value of hepatitis B virus precore and basal core promoter mutations in interferon-induced hepatitis B e antigen seroconversion.* Hepatology, 2013. **57**(3): p. 934-943.

68. Protzer, U., et al., *Antiviral activity and hepatoprotection by heme oxygenase-1 in hepatitis B virus infection.* Gastroenterology, 2007. **133**(4): p. 1156-1165.

69. Cardin, R., et al., *Oxidative damage in the progression of chronic liver disease to hepatocellular carcinoma: An intricate pathway.* World Journal of Gastroenterology, 2014. **20**(12): p. 3078-3086.

70. Ahn, S.H., et al., *Substitution at rt269 in Hepatitis B Virus Polymerase Is a Compensatory Mutation Associated with Multi-Drug Resistance.* Plos One, 2015. **10**(8).

71. Kim, H., et al., *Occult infection related hepatitis B surface antigen variants showing lowered secretion capacity.* World Journal of Gastroenterology, 2015. **21**(6): p. 1794-1803.

72. Kim, H., et al., *Discovery of a Novel Mutation (X8Del) Resulting in an 8-bp Deletion in the Hepatitis B Virus X Gene Associated with Occult Infection in Korean Vaccinated Individuals.* Plos One, 2015. **10**(10).

73. Kim, H., et al., *Preclinical Evaluation of In Vitro and In Vivo Antiviral Activities of KCT-01, a New Herbal Formula against Hepatitis B Virus.* Evidence-Based Complementary and Alternative Medicine, 2018.

국문초록

B 형 간염 바이러스 유전자형 C 의 역전사효소 내 rtL269I 변이주의 제 1 형 인터페론 신호전달을 통한 HBeAg 음성 감염 및 간질환 악화기전에 관한 연구

이소영

서울대학교 대학원

의학과 미생물학전공

지도교수 국윤호

B 형 간염 바이러스는 세계적으로 심각한 감염성 질환을 유발하며, 특히 B 형 간염 바이러스에 의한 만성 감염은 생명을 위협하는 간질환을 일으킨다. 그 중 유전자형 C 는 다른 유전자형에 비해 높은 병원성, 항바이러스제제 치료의 어려움, 인터페론 알파 치료의 저항성 및 간질환 악화의 급속한 진행 등의 특성이 관찰되었다. 이러한 특성은 유전자형 C 에서만 발견되는 여러 유전자 변이주 및 유전자 다형성에 기인할 가능성을 제시하는 연구가 보고되었으나, 특성과 관련된 근본적인 기전은 여전히 분명하게 밝혀진 바 없다. 본 연구에서는 유전자형 C 에서 HBV 중합효소 내 역전사

효소 rt269L 부위의 두가지 다형성 (rt269L 과 rt269I) 사이의 제 1 형 인터페론 (IFN-I)을 조절하는 특성과 감염 환자의 임상적 요인을 확인하였다. 이를 위하여 국내 유전자형 C rt269L과 rt269I에 감염된 환자 220명 사이의 임상적 요인을 비교하였으며, 감염환자 및 GenBank 데이터 베이스를 이용하여 두 다형성 사이의 preC 돌연변이 빈도를 분석하였다. 또한 임상적 특성의 원인을 규명하기 위하여 C57BL/6 마우스 및 간암세포 모델에서 감염시킨 후 바이러스 복제 양상, 제 1 형 인터페론 신호 기전 및 미토콘드리아 스트레스, 활성질소 등을 비교 관찰하였다.

본 연구의 임상 데이터를 통하여 rt269I 변이주가 rt269L 에 비하여 혈청 내 외피항원 (HBeAg) 음성감염, 낮은 수준의 HBV DNA 와 표면항원 (HBsAg), 그리고 질병의 악화를 야기하는 것을 확인하였다. 이러한 rt269I 감염에 의한 외피항원 음성감염은 preC 내 1896 번째 뉴클레오티드가 구아닌에서 아데노신으로 돌연변이가 생겨 일어나는 것임을 알 수 있었다. 또한 시험관 내 및 생체 내 연구에서는 rt269I 가 미토콘드리아 스트레스 매개 제 1 형 인터페론 생성을 유도하여 힘옥시게나제 (heme oxygenase)-1 의 발현을 증가시키고, 그 결과 HBV 복제를 감소시킬 수 있다는 것을 확인하였다. 또한, rt269I 변이주가 제 1 형 인터페론 의존적인 방식으로 산화질소활성효소 (inducible nitric oxide synthase) 매개 활성질소 생산을 향상시킬 수 있다는 것을 발견하였다.

이 연구를 통해 HBV 중합효소 내 역전사효소 부위에는 유전자형 C 에서만 발견되는 rt269L과 rt269I 두가지 다형성이 있음을 확인하였다. 뿐만 아니라, 이 연구의 결과는 rt269I 변이주가 미토콘드리아 스트레스 매개를 통해 제 1 형 인터페론을 생산하고, 이 기전이 만성감염 환자에서 외피항원 음성감염과 간 질환 악화에 영향을 줄 수 있음을 알 수 있었다.

중요어: B 형 간염 바이러스, 외피항원 음성감염, 유전형 C, 미토콘드리아 스트레스, 제 1 형 인터페론

학번: 2014-30594